CLASS
FRI

FILE COPY

REPORT NO. FRA/TTC-80/01

PB

DYNAMIC HOPPER CAR TEST

FAST Facility for Accelerated Service Testing

TRANSPORTATION TEST CENTER
PUEBLO, COLORADO 81001

MARCH 1980

INTERIM REPORT

This document is available to the public through
The National Technical Information Service,
Springfield, Virginia 22161

PREPARED FOR
THE FAST PROGRAM

AN INTERNATIONAL GOVERNMENT - INDUSTRY RESEARCH PROGRAM

U.S. DEPARTMENT OF TRANSPORTATION
FEDERAL RAILROAD ADMINISTRATION
Washington, D.C. 20590

ASSOCIATION OF AMERICAN RAILROADS
1920 L Street, N.W.
Washington, D.C. 20036

RAILWAY PROGRESS INSTITUTE
801 North Fairfax Street
Alexandria, Virginia 22314

RPI

3 - Rail Vehicles &
omponents

NOTICE

This document reflects events relating to testing at the Facility for Accelerated Service Testing (FAST) at the Transportation Test Center, which may have resulted from conditions, procedures, or the test environment peculiar to that facility. This document is disseminated for the FAST program under the sponsorship of the U. S. Department of Transportation, the Association of American Railroads, and the Railway Progress Institute in the interest of information exchange. The sponsors assume no liability for its contents or use thereof.

NOTICE

The FAST program does not endorse products or manufacturers. Trade or manufacturers' names appear herein solely because they are considered essential to the object of this report.

Technical Report Documentation Page

1. Report No.	2. Government Accession No.	3. Recipient's Catalog No.
FRA/TTC-80/01		

4. Title and Subtitle	5. Report Date
Dynamic Hopper Car Test	March 1980
	6. Performing Organization Code
	8. Performing Organization Report No.
7. Author(s)	DOT-FR-77-21
M. Kenworthy and C.T. Jones	
9. Performing Organization Name and Address	10. Work Unit No. (TRAIS)
Engineering Test and Analysis Division ENSCO, INC. 2560 Huntington Ave. Washington, DC 20590	11. Contract or Grant No. DOT-FR-64113
	13. Type of Report and Period Covered
12. Sponsoring Agency Name and Address	Interim Report
U.S. Department of Transportation* Federal Railroad Administration 2100 Second Street, S.W. Washington, DC 20590	14. Sponsoring Agency Code

15. Supplementary Notes

*Edited and Approved by
Facility for Accelerated Service Testing Program
Transportation Test Center, Pueblo, Colorado 81001

16. Abstract

This report describes a test designed to establish the relationship between ride performance and track degradation, vehicle component wear, and the combined effect of rail degradation and component wear. The test was also designed to quantify the dynamic response of freight vehicles to different track structures.

Two 100-ton hopper cars, one a high-mileage car and the other a low-mileage car, were instrumented and used to measure lateral and vertical wheel/rail forces, and truck and carbody modal accelerations.

The results of the test will be used to quantify the dynamic response of freight vehicles to different track structures and to establish a baseline for future study of ride performance, and track and vehicle degradation.

17. Key Words		18. Distribution Statement
Hopper Cars	Vehicle Component	Document is available to the public through
Dynamic Test	Wear	National Technical Information Service
Wheel-Rail Forces		Springfield, VA 22161
Ride Performance		
Track Degradation		

19. Security Classif. (of this report)	20. Security Classif. (of this page)	21. No. of Pages	22. Price
Unclassified	Unclassified	75	

Form DOT F 1700.7 (8-72) Reproduction of completed page authorized

METRIC CONVERSION FACTORS

Approximate Conversions to Metric Measures

Symbol	When You Know	Multiply by	To Find	Symbol
		LENGTH		
in	inches	2.5	centimeters	cm
ft	feet	30	centimeters	cm
yd	yards	0.9	meters	m
mi	miles	1.6	kilometers	km
		AREA		
in^2	sq inches	6.5	sq centimeters	cm^2
ft^2	sq feet	0.09	sq meters	m^2
yd^2	sq yards	0.8	sq meters	m^2
mi^2	sq miles	2.6	sq kilometers	km^2
	acres	0.4	hectares	ha
		MASS (weight)		
oz	ounces	28	grams	g
lb	pounds	0.45	kilograms	kg
	short tons (2000 lb)	0.9	tonnes	t
		VOLUME		
tsp	teaspoons	5	milliliters	ml
tbsp	tablespoons	15	milliliters	ml
fl oz	fluid ounces	30	milliliters	ml
c	cups	0.24	liters	l
pt	pints	0.47	liters	l
qt	quarts	0.95	liters	l
gal	gallons	3.8	liters	l
ft^3	cubic feet	0.03	cubic meters	m^3
yd^3	cubic yards	0.76	cubic meters	m^3
		TEMPERATURE (exact)		
^oF	Fahrenheit	5/9 (after subtracting 32)	Celsius	^oC

Approximate Conversions from Metric Measures

Symbol	When You Know	Multiply by	To Find	Symbol
		LENGTH		
mm	millimeters	0.04	inches	in
cm	centimeters	0.4	inches	in
m	meters	3.3	feet	ft
m	meters	1.1	yards	yd
km	kilometers	0.6	miles	mi
		AREA		
cm^2	sq centimeters	0.16	sq inches	in^2
m^2	sq meters	1.2	sq yards	yd^2
km^2	sq kilometers	0.4	sq miles	mi
ha	hectares (10,000 m)	2.5	acres	a
		MASS (weight)		
g	grams	0.035	ounces	oz
kg	kilograms	2.2	pounds	lb
t	tonnes (1000 kg)	1.1	short tons	
		VOLUME		
ml	milliliters	0.03	fluid ounces	fl oz
l	liters	2.1	pints	pt
l	liters	1.06	quarts	qt
l	liters	0.26	gallons	gal
m^3	cubic meters	35	cubic	ft
m^3	cubic meters	1.3	cubic	yd
		TEMPERATURE (exact)		
^oC	Celsius	9/5 (then add 32)	Fahrenheit	^oF

TABLE OF CONTENTS

TABLE OF CONTENTS, CONTINUED.

LIST OF TABLES

LIST OF FIGURES

LIST OF FIGURES, CONTINUED.

This page left blank intentionally.

EXECUTIVE SUMMARY

It is reasonable to assume that the dynamic performance of the railcar/track system will degrade with accumulated mileage and tonnage. The overall objectives of the program described in this report were to establish the relationship between ride quality and track condition, vehicle component wear, and the combined effects of track and component wear. Specific objectives were to:

- Establish the relationship between ride performance and track degradation with usage.
- Establish the relationship between ride performance and vehicle component wear with usage.
- Establish the relationship between ride performance and the combined effect of rail degradation and vehicle component wear.
- Quantify the dynamic response of freight vehicles to different track structures.

Following the methodology adopted for this study, the test series described in this report was conducted to establish a baseline from which subsequent test series would be conducted to address the specific program objectives.

For the purpose of this program, two 100-ton hopper cars from the FAST program were designated for this study. One car continued normal operation in the FAST consist, referred to as the high-mileage car, while the other, referred to as the control car, was not operated in any consist. Each vehicle was instrumented identically with accelerometers to measure the dynamic behavior as the FAST loop was negotiated at 30 to 40 mi/h and at five equally spaced speeds between 10 mi/h and 50 mi/h over a specially selected portion of the Railroad Test Track. Five 5 g linear accelerometers were mounted on each carbody in such a manner as to allow the extraction of the most generalized mode response of the carbody including sway (lateral), bounce (vertical), roll, pitch, and yaw accelerations. Similarly, six 30 g linear accelerometers were mounted to the leading truck of each car from which the same five rigid body modes were obtained with the addition of a quasielectric body mode referred to as twist. Twist may be thought of as the out-of-phase roll of the truck axles. Wheel/rail force measurements were taken using an AAR-supplied instrumented wheelset capable of measuring vertical and lateral forces simultaneously on the trailing axle of the trailing truck. Precision speed and location signals were recorded to aid in data processing. Some limited additional accelerometers and displacement transducer signals were also recorded but are not reported herein.

The four specific program objectives will be addressed as follows. In order to establish the relationship between ride performance and track degradation, the performance of the control car will be monitored as the FAST loop accumulates tonnage. The relationship between vehicle component wear and ride performance will be established through repeated measurements of the high-mileage car over the RTT test zone. The combined effects of vehicle component and track wear will be studied by observing the performance of the

high-mileage car over the FAST loop at specified intervals of time. Finally, the response of freight vehicles to different track structures will be determined primarily through measurements taken on the control car operating on the FAST loop. Additional information can also be obtained from the high-mileage car over the FAST loop.

It should be pointed out that no comparisons between cars are made due to the fact that the cars designated for this project were of slightly different design and were equipped with different types of trucks. Some observations are made in this report as to relative performance, but these are not meant as wear-related assessments. Because of the nature of the program methodology, the results of this report are directed primarily at the fourth objective, the quantification of the dynamic response of freight vehicles to different track structures. Conclusions related to this objective are as follows.

Variations in track structure, such as ballast-shoulder width and depth, spiking patterns, tie material, and rail anchors, had little if any effect on truck and carbody accelerations or wheel force. In contrast, curves greater than 4^{o}, and discrete events such as turnouts, had a marked effect on vehicle dynamics. Section 05 of the FAST Track, containing unsupported bonded joints, produced the highest carbody accelerations, while truck mode accelerations over this same section of track were moderate to low.

Future dynamic tests will be conducted which will address the three remaining objectives, all of which are wear related and, therefore, require additional accumulation of mileage on both the vehicle and track.

1.0 INTRODUCTION

Dynamic performance of the railroad car/track system changes substantially with accumulated mileage. These changes are caused primarily by the degradation of track structures and vehicle components with tonnage and mileage. As a result, economic losses are incurred due to increased lading damage and track and vehicle maintenance.

The dynamic hopper car test is part of Phase I of the Facility for Accelerated Service Testing (FAST) Program being conducted at the Transportation Test Center (TTC), Pueblo, Colorado. The goal of the dynamic hopper car test is to determine the relationship between the dynamic performance of freight vehicles, accumulated mileage, and track structures. Specific objectives are to:

- Establish the relationship between ride performance and track degradation with usage,
- Establish the relationship between ride performance and vehicle component wear with usage,
- Establish the relationship between ride performance and the combined effect of rail degradation and vehicle component wear, and
- Quantify the dynamic response of freight vehicles to different track structures.

In order to meet the objectives listed above, two 100-ton hopper cars were selected for testing. One car, designated the "high-mileage" car, is operated in the FAST consist at an accelerated service rate. The second hopper car, designated the "low-mileage" or control car, is utilized to determine the effects of track degradation independent of component wear.

Both cars are to be instrumented at specified intervals of accumulated mileage and operated over the FAST Track and sections of the TTC Railroad Test Track (RTT). For the results presented in this report, instrumentation on the high-mileage car consisted of accelerometers mounted on one truck and the carbody. The low-mileage car was instrumented with accelerometers in a similar manner and the B-end* truck was equipped with two instrumented wheelsets to measure lateral and vertical wheel-to-rail forces.

The data contained in this report will provide a baseline for establishing the relationships between ride performance and track and component wear. The data will be used directly to quantify vehicle dynamic response to differing track structures and will serve as the initial data base for subsequent comparative analysis.

---

* B-end = Brake end of car.

2.0 TEST DESCRIPTION

2.1 GENERAL

Dynamic data were obtained from two 100-ton hopper cars as they were operated at speeds ranging from 10 to 50 mi/h over the test zones. This section provides a detailed description of the vehicles, test procedures, consists, test zones, and instrumentation used to obtain dynamic data.

2.2 TEST ZONES

Testing was conducted at the TTC on two separate test zones. Figure 2-1 is a plan of the TTC. The primary test zone is the 4.8-mile FAST Track. This track (figure 2-2) is comprised of a total of 22 separate track test sections which contain different types of construction. The secondary test zone was a 3,530-ft portion of the RTT. This test zone is comprised of conventional bolted rail, with 136 lb/yd rail on wooden ties with 19-1/2" centers.

The test zone on the RTT extended from station 370+30 to station 335+00, a distance of 3,530 ft. Three automatic location detector (ALD) targets (10 ft apart) were placed at the beginning of the zone (station 335+00). Two targets were placed at the center of the zone, and two at the end of the zone. On the FAST Track, ALD targets were placed at the beginning of each section. Table 2-1 lists the relevant station locations. Targets are generally located at the beginning and end of each section. For a more detailed description of FAST see reference 2.

2.3 TEST VEHICLES

Two test vehicles, both 100-ton hopper cars, were used for this test. They were car 46 and car 47, shown in figures 2-3 and 2-4. Car 47 was used as the low-mileage (500 FAST miles) or control vehicle, while car 46 was subjected to accelerated service conditions in the FAST consist and, as a result, had accumulated 15,200 mi of service on FAST. The number of miles these cars had seen in revenue service previously is not known. Car 47 is identified as CEI car No. 588435, and car 46 is B&O car No. 163813. The two car dimensions were essentially the same. Certain relevant nominal dimensions are listed in table 2-2.

Although the carbodies of the two vehicles were quite similar, they were equipped with different trucks. Car 46 was equipped with a Barber S-2 truck, while car 47 had an ASF Ride Control truck with seven D-5 outer springs, seven

---

[2] The FAST Track, Facility for Accelerated Service Testing, AAR Technical Center, Chicago, Illinois, September, 1976.

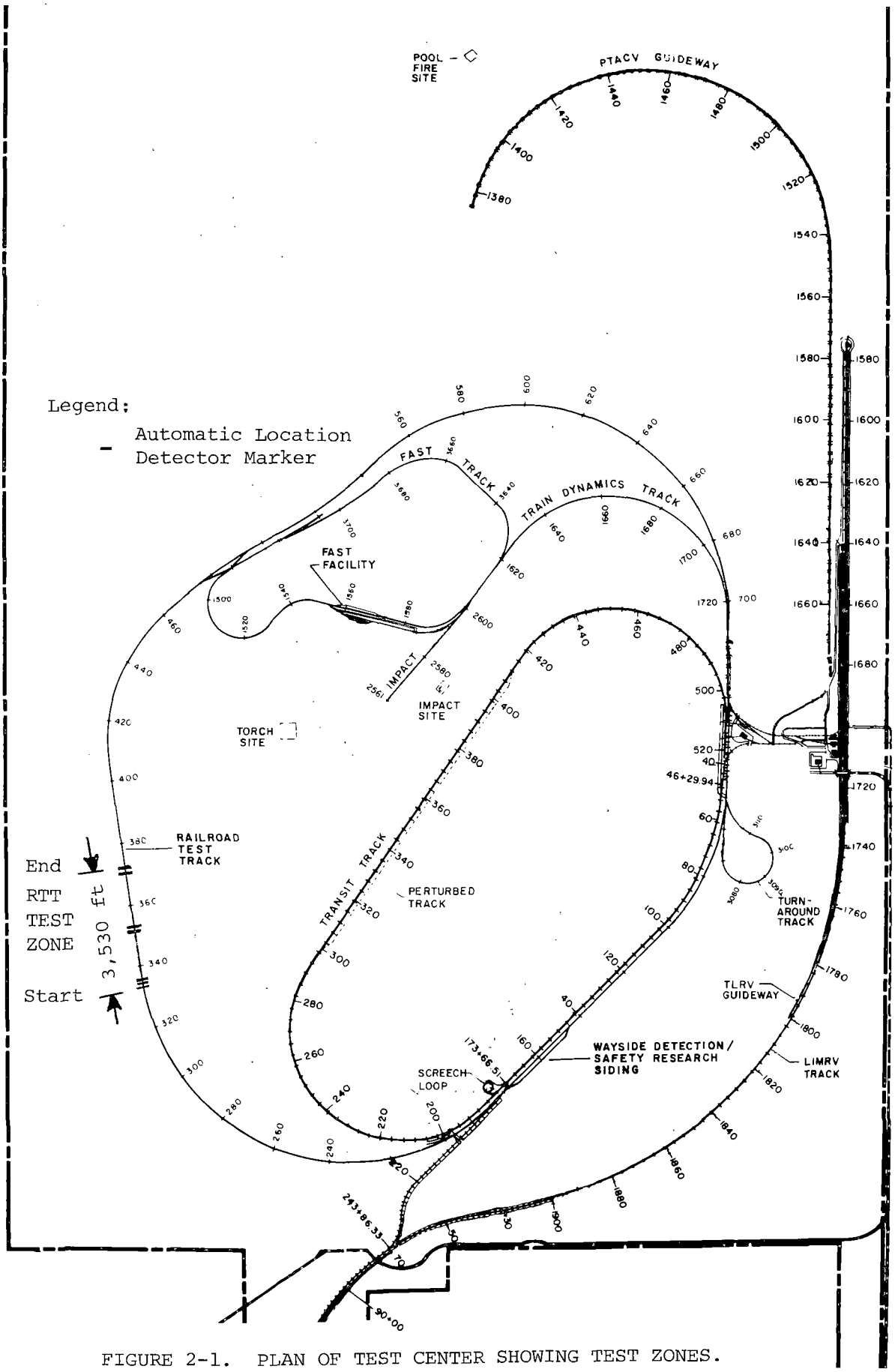

FIGURE 2-1. PLAN OF TEST CENTER SHOWING TEST ZONES.

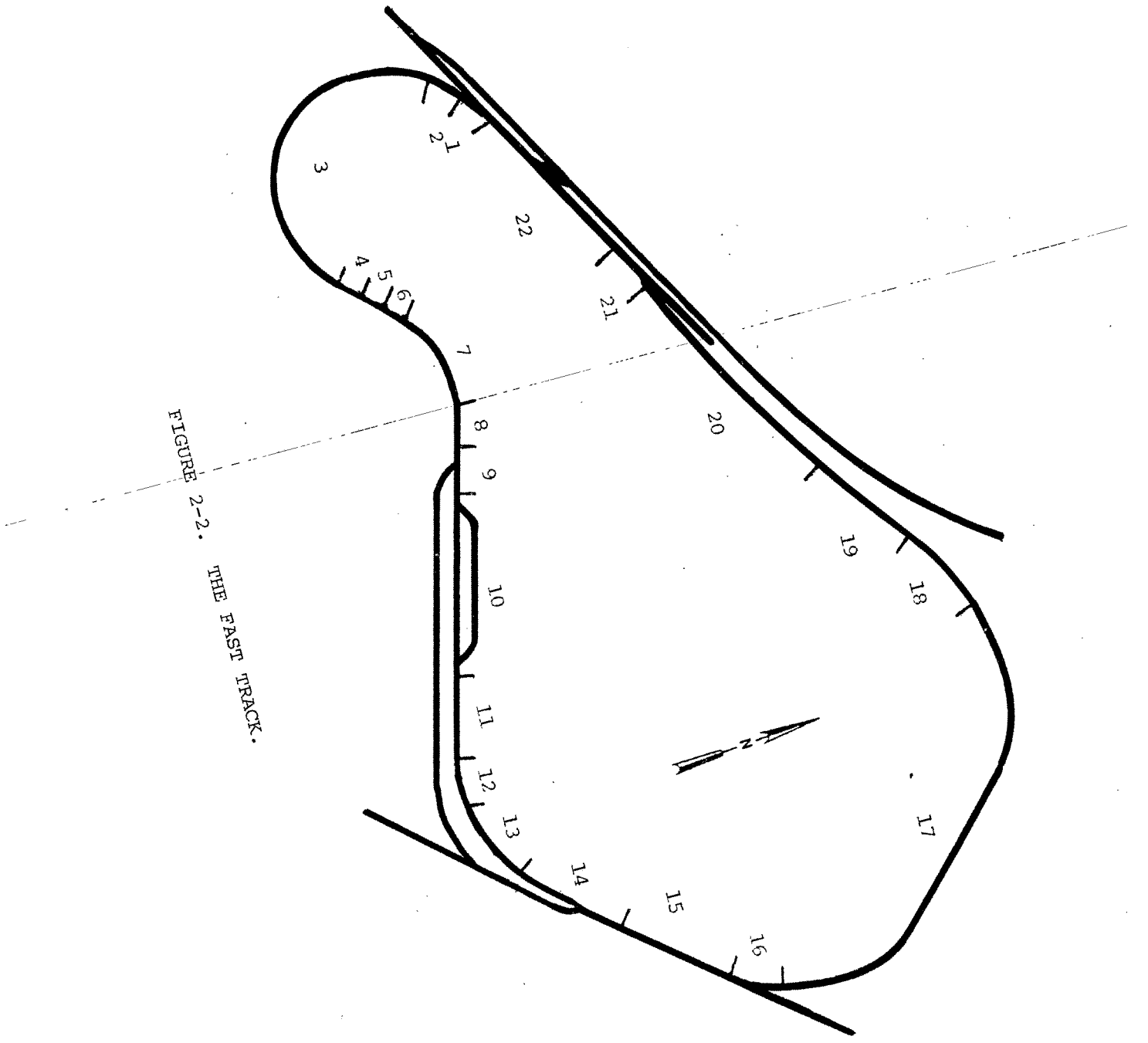

FIGURE 2-2. THE FAST TRACK.

TABLE 2-1. FAST TRACK STATION NUMBERS.

Section	Length (ft)		Station Numbers		
01	170.00		1487+50.00	to	1489+20.00
02	329.30 (Begin CWR)		1489+20.00	to	1492+49.30
03	3,736.70	Segment A	1492+49.30	to	1496+23.30
		B	1496+23.30	to	1499+97.30
		C	1499+97.30	to	1503+71.30
		D	1503+71.30	to	1507+45.00
		E	1507+45.00	to	1511+19.30
		F	1511+19.30	to	1514+94.00
		G	1514+94.00	to	1518+68.50
		H	1518+68.50	to	1522+42.00
		I	1522+42.00	to	1526+12.50
		J	1526+12.50	to	1529+86.00
04	214.00		1529+86.00	to	1532+00.00
05	222.02		1532+00.00	to	1534+22.02
06	300.00		1534+22.02	to	1537+22.02
07	1,000.98	Segment A	1537+22.02	to	1539+23.00
		B	1539+23.00	to	1541+23.00
		C	1541+23.00	to	1543+22.90
		D	1543+22.90	to	1545+21.60
		E1	1545+21.60	to	1546+20.50
		E2	1546+20.50	to	1547+23.00
08	299.02 (CWR ends 1549+40.00)		1547+23.00	to	1549+40.00
			1549+40.00	to	1550+22.02

TABLE 2-1. FAST TRACK STATION NUMBERS, CONTINUED.

Section	Length (ft)		Station Numbers		
09	562.44	Conventional ties	1550+22.02	to	1550+64.00
		Reconstituted ties	1550+64.00	to	1551+97.50
		Conventional ties	1551+97.50	to	1553+70.00
		Dowel ties	1553+70.00	to	1555+34.00
		Conventional ties	1555+34.00	to	1555+84.46
10	1,681.08	Turnout	1555+84.46	to	1558+12.46
			1558+12.46	to	1570+37.54
		Turnout	1570+37.54	to	1572+65.54
11	844.46		1572+65.54	to	1581+10.00
12	324.00		1581+10.00	to	1584+34.00
13	1,248.00 (CWR)		1584+34.00	to	1596+82.00
14	877.54		1596+82.00	to	1604+05.00
		Turnout	1604+05.00	to	1605+59.54
15	1,180.92		1605+59.54	to	1606+00.00
		6" wide shoulder	1606+00.00	to	1611+50.00
		18" wide shoulder	1611+50.00	to	1617+00.00
			1617+00.00	to	3617+40.46
16	222.00		3617+40.46	to	3619+62.46
17	6,150.85 (CWR)		3619+62.46	to	3620+84.60
		Subsection A	3620+84.60	to	3626+14.00
		B	3626+14.00	to	3629+38.50
		C	3629+38.50	to	3632+64.70
		D1	3632+64.70	to	3635+81.20
		D2	3635+81.20	to	3637+89.30

TABLE 2-1. FAST TRACK STATION NUMBERS, CONTINUED.

Section	Length (ft)		Station Numbers		
17 (continued)		Subsection E	3637+89.30	to	3641+85.50
		F	3641+85.50	to	3643+87.50
		G	3643+87.50	to	3648+97.00
		H1	3648+97.00	to	3652+52.20
		H2	3652+52.20	to	3655+86.50
		I-1-1	3655+86.50	to	3657+10.50
		I-1-2	3657+10.50	to	3658+37.50
		I-2	3658+37.50	to	3660+07.50
		J1	3660+07.50	to	3664+49.50
		J2	3664+49.50	to	3667+65.00
		K-1-1	3667+65.00	to	3668+13.50
		K-1-2	3668+13.50	to	3669+49.50
		K-2	3669+49.50	to	3673+13.50
		L	3673+13.50	to	3679+13.50
			3679+13.50	to	3681+13.31
18	821.79	Segment A	3681+13.31	to	3684+75.00
		B	3684+75.00	to	3689+35.10
19	600.00	Segment A	3689+35.10	to	3692+35.10
		B	3692+35.10	to	3695+35.10
20	2,331.60	Segment A	3695+35.10	to	3698+50.00
		B	3698+50.00	to	3699+64.10
		B1	3699+64.10	to	3701+59.10
		C	3701+59.10	to	3704+71.10
		D	3704+71.10	to	3706+30.00

TABLE 2-1. FAST TRACK STATION NUMBERS, CONTINUED.

Section	Length (ft)		Station Numbers		
20 (continued)		Segment D1	3706+30.00	to	3707+83.00
		E	3707+83.00	to	3709+50.00
		E1	3709+50.00	to	3711+00.00
		F	3711+00.00	to	3714+07.10
		G	3714+07.10	to	3718+22.20
			3718+22.20	to	3718+66.70
21	177.50		3718+66.70	to	3720+44.20
22	1,893.50 (CWR)		506+43.50	to	505+19.50
		Segment A	505+19.50	to	502+25.00
		A1	502+25.00	to	501+75.20
		B	501+75.20	to	498+81.20
		C	498+81.20	to	495+71.50
		D	495+71.50	to	492+25.00
		E	492+25.00	to	488+50.00
			488+50.00	to	487+50.00

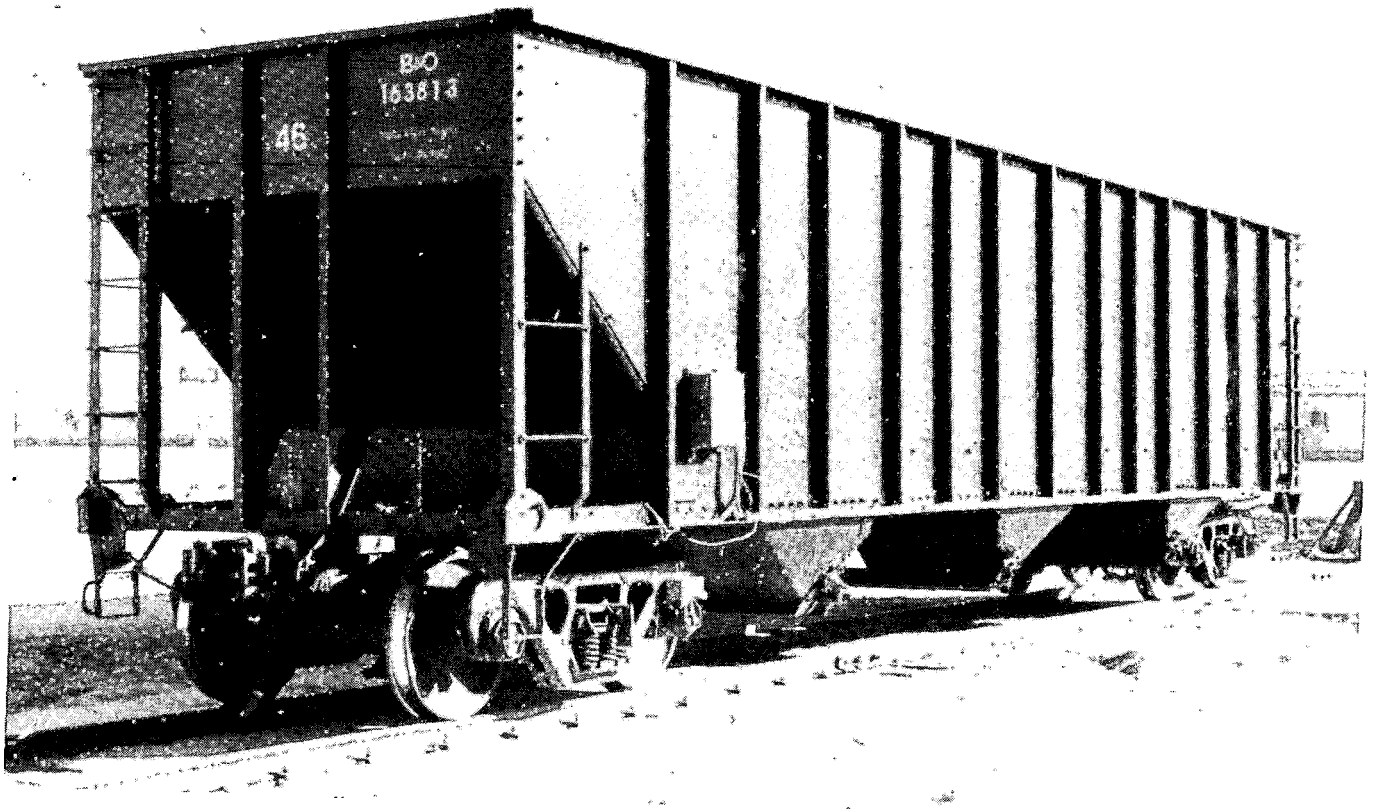

FIGURE 2-3. TEST CAR 46 - HIGH-MILEAGE VEHICLE WITH BARBER S-2 TRUCK.

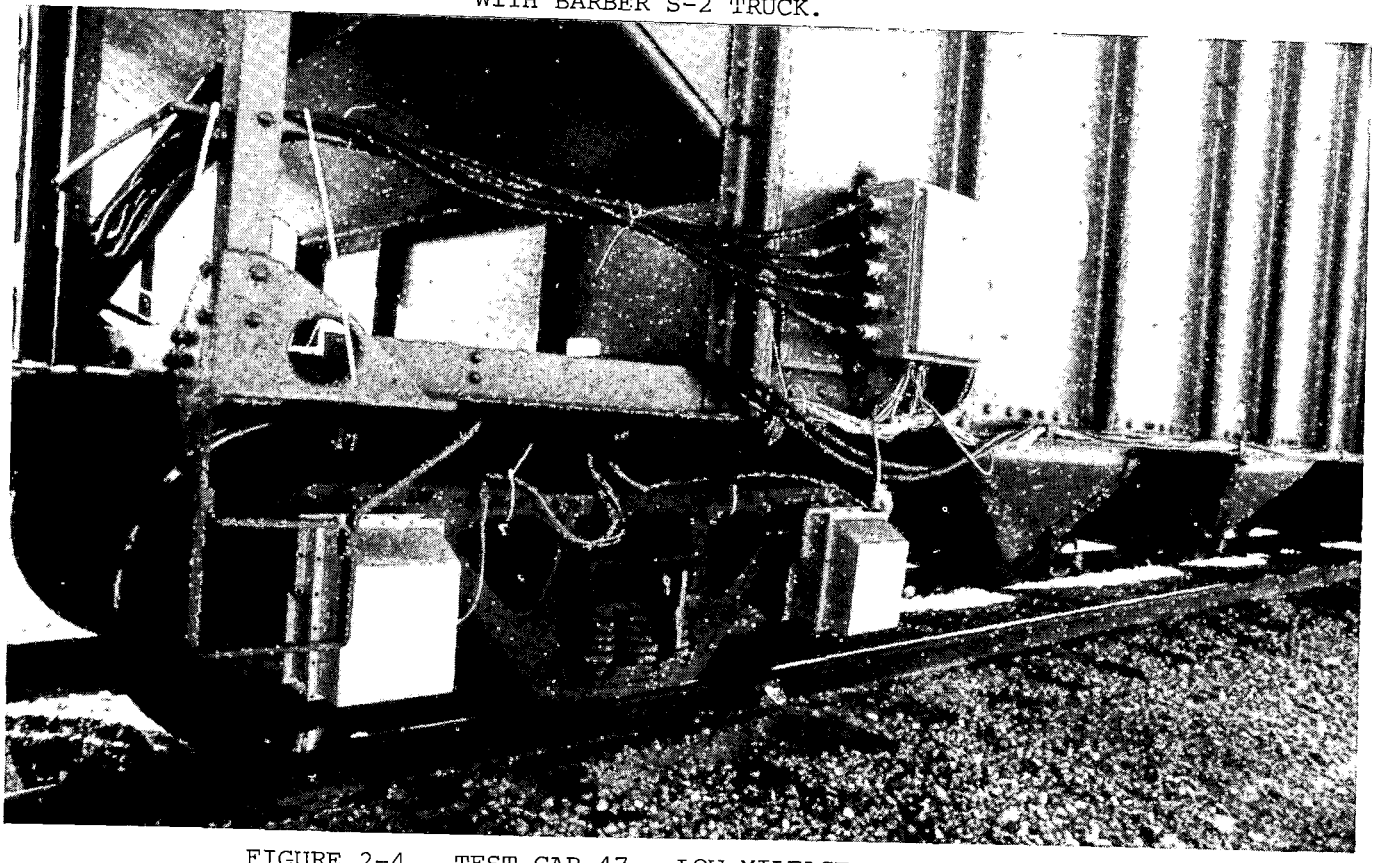

FIGURE 2-4. TEST CAR 47 - LOW-MILEAGE VEHICLE WITH ASF RIDE CONTROL TRUCK AND INSTRUMENTED TRUCK.

TABLE 2-2. RELEVANT DIMENSIONS OF 100-TON HOPPER CARS.

DESCRIPTION	DIMENSION	
Carbody length	46	ft
Carbody width	10.25	ft
Carbody height	7.9	ft
Car weight (gross)	262,000	lb
Truck length	5.83	ft
Truck width	7.47	ft
Truck distance (center to center)	39.25	ft
Bolster width	8	ft

D-5 inner springs, and two stabilizers in each group. The S-2 truck had seven each of inner and outer D-5 springs. Car 46 had 16" center plates while car 47 had 14" center plates. Both were equipped with conventional side bearings and 6-1/2" x 12" roller bearings.

One truck on car 47 was instrumented to measure vertical and lateral wheel forces. This installation did not produce major structural modifications and the wheel/axle set could be considered equivalent to any uninstrumented set.

2.4 INSTRUMENTATION

Accelerometers and strain gage force transducers were installed at key points on the vehicle. The analog signals from these transducers were cabled directly from the test vehicle to the data acquisition car, T-5. The signals were then conditioned and recorded in digital form on magnetic tape using a digital-computer-based data acquisition system. A total of 38 signals were recorded. Of these signals, 20 were acceleration, 16 were force, one was speed, and one was location.

Figure 2-5 is a more detailed block diagram of the system. The vehicle was equipped with accelerometers, an ALD system, a wheel position encoder, and four strain gaged wheels to obtain vertical and lateral forces. The output signals from the accelerometers and the strain gages were in analog form while the ALD and encoder signals were digital.

An ENSCO fabricated accelerometer signal conditioning chassis provided $\pm$15 V d.c. excitation to the accelerometers and provided a means for zeroing and scaling these signals. The conditioned signals were then anti-alias filtered by a four-pole, low-pass, Bessel function filter with the cutoff frequency set at 30 Hz. Filtered signals were routed to an analog multiplexer and converted to digital form at a rate of 128 samples per second. The digital data were recorded for subsequent processing on magnetic tape. As a partial check on the integrity of the recording system, the incoming digitized data were reconverted to analog form by the D/A converter. Selected channels of converted analog data were displayed on an 8-channel analog recorder. The D/A system also provided a convenient means for regenerating and viewing recorded test data.

Strain gages on four wheels on the control car were excited from strain gage signal conditioning amplifiers in T-5. The same amplifiers provided a means for adjusting scale factors and zeroing the strain gage outputs. Conditioned strain gage signals were filtered and converted to digital form in the same manner as accelerometer signals. In addition to the analog force signals, a wheel position signal was also recorded to provide a means for correlating wheel rotational position with the force signals during subsequent data processing.

Location of the test vehicle along the track was determined by a capacitive sensor located on the test vehicle. The sensor detected the presence of steel objects between the rails and provided a voltage pulse whenever an object was sensed. This provided correlation between particular events in the data and distance along the track.

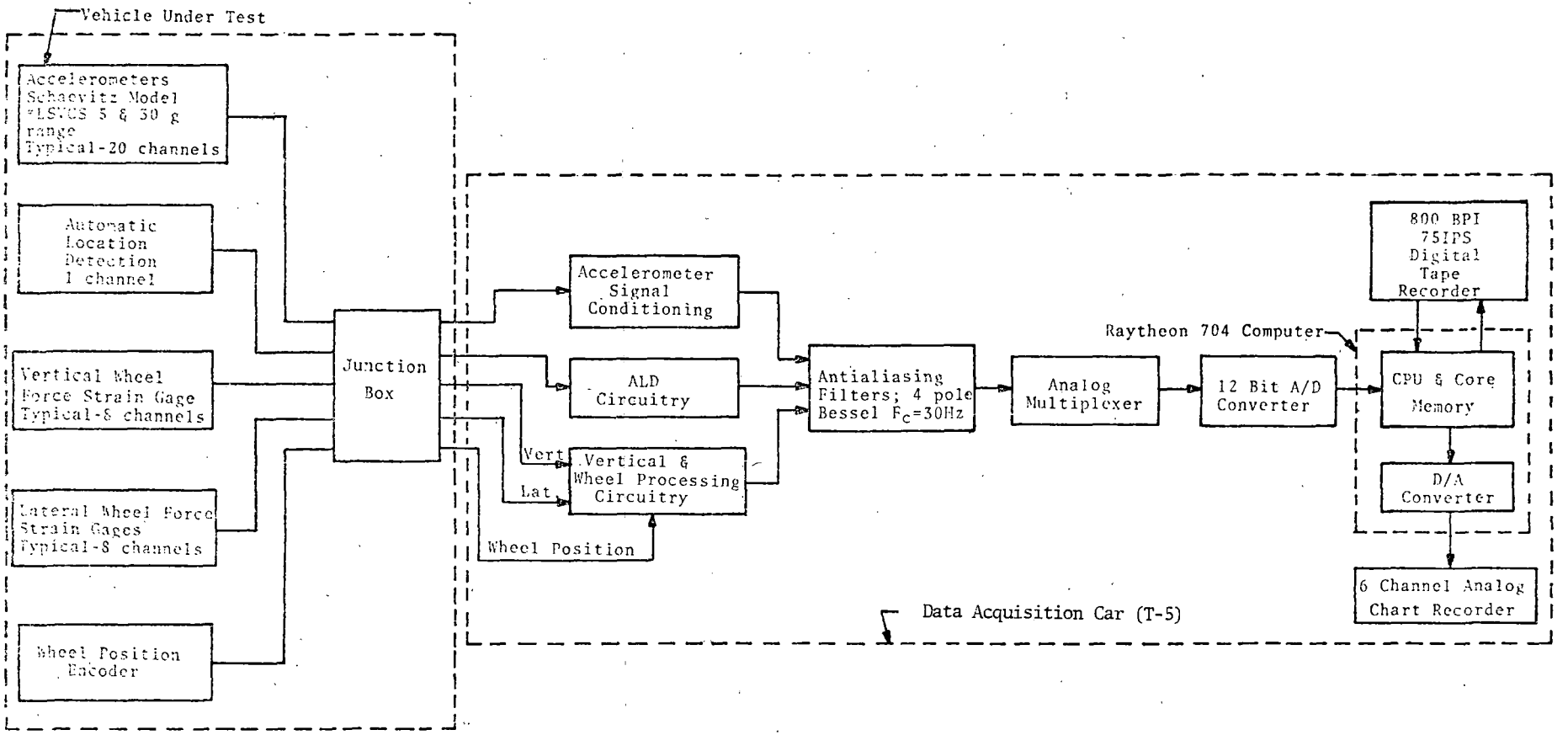

FIGURE 2-5. DETAILED BLOCK DIAGRAM OF DATA SYSTEM.

An analog speed signal, which was generated by the speed measurement system on T-5, was also recorded.

2.4.1 Accelerometers

Twenty accelerometers were mounted at various points on the truck and carbody of the test vehicle. The accelerometers on the truck were 30 g units, Schaevitz Model No. LSVCS, while those on the carbody were 5 g versions of the same unit. This basic accelerometer was the force balance servo type with natural frequencies between 25 and 30 Hz.

The vehicle acceleration environment was relatively severe with frequent high-amplitude/high-frequency accelerations present. These accelerations were potentially damaging to the accelerometers and for the purposes of this test were not of interest. To reduce the effect of these undesirable accelerations, a special acceleration mounting technique was used. Basically, the mounting technique imposed a mechanical filter between the structure (the acceleration of which is being measured) and the accelerometer. The mechanical filter attenuated frequencies above 150 Hz at a rate of about 12 dB per octave. This attenuation of higher frequencies allowed the use of relatively sensitive accelerometers in an acceleration environment which would otherwise have saturated or destroyed them. A more detailed description of this mounting technique is contained in reference 3.

2.4.2 Lateral and Vertical Wheel Force Measurement

Wheels on two wheel/axle sets were instrumented with strain gages to obtain lateral and vertical wheel forces. The gages were applied to the plate of the wheel (figure 2-6), and the output signals from the gages were brought out via slip rings.

The analog output signals were digitized for subsequent processing by a digital computer. Additional processing was required because the vertical wheel force signals are essentially periodic rather than constant. Two such periodic wheel force signals, displaced by 90° of wheel rotation, were generated, providing four peak output signals per wheel revolution as shown in figure 2-7. Only the peak values were used as a measure of vertical wheel force because they provided maximum sensitivity.

The lateral force signals were essentially continuous and possessed a nearly constant scale factor. As a result, only signal conditioning was required and peak detection was not used during subsequent processing. A complete description of the instrumented wheelset is contained in reference 4.

---

[3] Letter providing technical information on application of servo accelerometers, Robert D. Christian, ENSCO, Inc., to John C. Mould, FRA, May 11, 1976.

[4] Instrumentation for Measurement of Forces on Wheels of Rail Vehicles, Report FRA-ORD&D-75-11, May 1974.

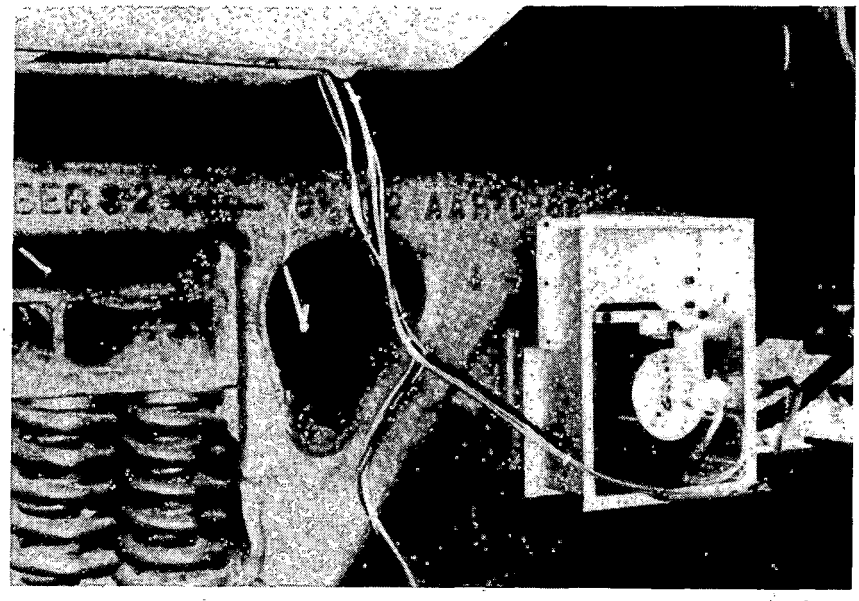

FIGURE 2-6. INSTALLED POSITION OF SLIP RING ASSEMBLY AND ENCODER.

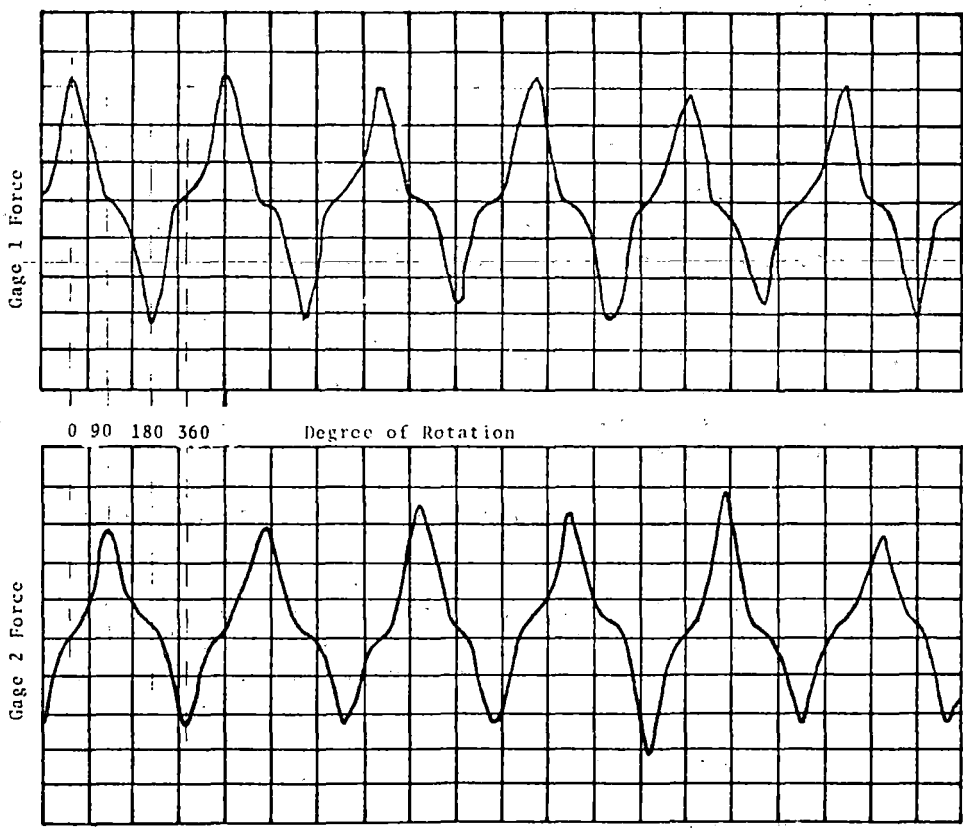

FIGURE 2-7. TWO HARMONIC WHEEL FORCE SIGNALS WITH PEAKS FROM GAGE 1 TO GAGE 2 DISPLACED BY 90°.

2.4.3 Speed and Location

Accurate speed and location signals were recorded simultaneously with other measured quantities so that during subsequent data processing, the speed and location of the test vehicle at any given instant during the test could be determined.

2.4.3.1 Speed. Speed was measured on the T-5 car rather than the test vehicle, primarily for convenience. The T-5 car was equipped with a 1000-pulse-per-revolution optical shaft encoder which was mechanically driven by the car wheel. The output of the encoder was a pulse train whose frequency was proportional to car speed. This pulse train was connected to a frequency-to-direct-current converter whose output was a d.c. voltage proportional to input frequency.

2.4.3.2 Automatic location detector. The ALD is a commercially available metal detecting device modified for test use. The sensing head was mounted at the center of the test vehicle and connected to conditioning electronics located in T-5. The device was adjusted so that the electronics provided a high voltage level as its output whenever substantial metal objects passed under the head. Correspondingly, the absence of metal under the head produced a low voltage level at the output. When passing over such items as switches, crossover rails, etc., the ALD produced voltage pulses which provided a means of determining the exact location of the test consist on the track.

Additionally, individual test sections were marked with metal targets which provided output pulses suitable for identification of those test sections. Figure 2-8 shows one of the targets in place.

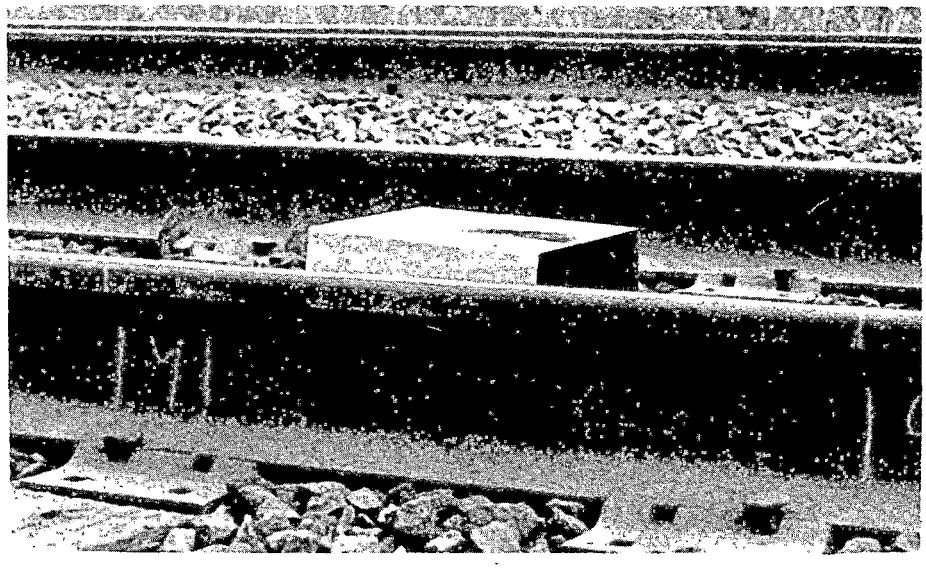

FIGURE 2-8. TYPICAL ALD TARGET IN PLACE.

2.4.4 Calibration

Calibration of each measurement channel was performed prior to and after each day of testing. The procedures used for each calibration are described in the following sections.

2.4.4.1 Accelerometers. Accelerometers were calibrated using the turnover technique in which the accelerometer was rotated to subject it to the effects of the earth's gravitational field. Initially, the accelerometer was oriented so that its sensitive axis was subjected to 1.0 g. Then it was rotated 90° or 180° to obtain a 1.0 g or 2.0 g change in acceleration. Certain of the 5.0 g range accelerometers were biased 1.0 g to offset the effect of the earth's gravitational field. These accelerometers were oriented vertically and then rotated 90° to obtain a 1.0 g change. The unbiased 5.0 g range units were oriented vertically and rotated 180° to obtain a $\pm$ 1.0 g or 2.0 g total change.

During the rotation, the output levels of the accelerometer signal conditioners were recorded on digital magnetic tape to provide zero and calibration levels during subsequent processing. In addition, the signals were measured and recorded on calibration sheets. Also the signals were recorded in analog form on the Brush chart recorder to provide a permanent record.

2.4.4.2 Lateral and vertical wheel force measurements. Two different methods were utilized to calibrate the wheel force measurement systems:

Vertical - Calibration of the vertical force channels made use of the fact that, on the average, the car exerted a known force on an individual wheel. The car weighed approximately 262,000 pounds and because of the relative freedom in the truck, each wheel carried one-eighth of the car weight or 33,000 pounds.

For calibration, the test vehicle was moved until the wheelset was positioned so that a null was obtained in the output from the wheel being calibrated. The signal conditioner was adjusted to provide zero output. The vehicle was then moved until the wheelset strain gages provided a maximum output. The gain of the amplifier was then adjusted to obtain 3.30 volts on a scale factor of 10,000 lbs/V. This procedure was repeated for all eight vertical force measurement channels.

Lateral - A convenient method for applying a known lateral load to the wheelsets was not available. As a result, shunt resistors were used for calibration. After a channel was zeroed, the shunt resistors were connected across the bridge and the amplifier gain was adjusted to obtain 4.00 volts, which corresponded to 30,000 pounds or a scale factor of 7,500 lbs/V.

The calibration resistor values were determined in the laboratory during initial gage installation by applying a known lateral load and noting the resulting output. This same output was then obtained by shunting the bridge with the appropriate resistor. As a cross-check, the test car was parked on a known superelevation and the lateral force component seen by the wheelset

was computed and compared fairly well with the electronically measured quantity.

2.4.4.3 Speed and location. The speed measurement system is an integral part of the data acquisition car T-5 and seldom requires calibration. Periodic calibration is performed by towing the vehicle over a known distance which is marked by ALD targets. The ALD signals are used to open and close gates on an electronic counter which accumulates the number of pulses obtained from the wheel-driven encoder over the known distance. From this quantity, the number of pulses per foot traveled is calculated and set into the speed and distance processor.

ALD measurements indicate the presence or absence of substantial amounts of metal. Calibration was performed by moving a metal object, such as a shovel, near the face of the detector mounted on the truck. Proper setup of the instrument was indicated by a signal level change at the output of the detector whenever the object was moved close to or away from the detector.

2.5 CONVENTIONS AND DEFINITIONS

A consistent set of conventions and definitions was adopted for vehicle components, data channels, and reference axes used in this test.

Figures 2-9 and 2-10 illustrate the conventions used for the two cars. Note that the B-end always led in the direction of travel. The left side of the car was the side to the viewer's right when he faced the direction of travel. Major structural components such as axles and transducers are included. Accelerometer locations were indicated by the letters O, L, and V in small boxes, denoting the direction of the measurement, longitudinal, lateral, and vertical, respectively. The letter E enclosed in a similar box indicated the locations of the wheel position encoders.

In order to locate a specific transducer on a truck, the side of the truck was indentified first by the letters L or R for left or right, determined by standing at the B-end and facing the A-end. This letter was followed by a second letter or number indicating whether the location was on a bolster or an axle. The bolsters were labeled A or B according to their position on the A-end or the B-end of the car. Axles were numbered 1 through 4 starting with the outboard axle of the B-end truck.

Carbody accelerometers were located with a series of three letters. The first letter was B, indicating that the accelerometer was located in the carbody. The second letter indicated the A-end or B-end, as defined above. The third letter indicated the location relative to the carbody centerline: L denoting left, C denoting on the centerline, and R denoting right. For example: R1 was the accelerometer on the right side, leading journal on the B-end axle; BAC was the accelerometer on the carbody, A-end, center location.

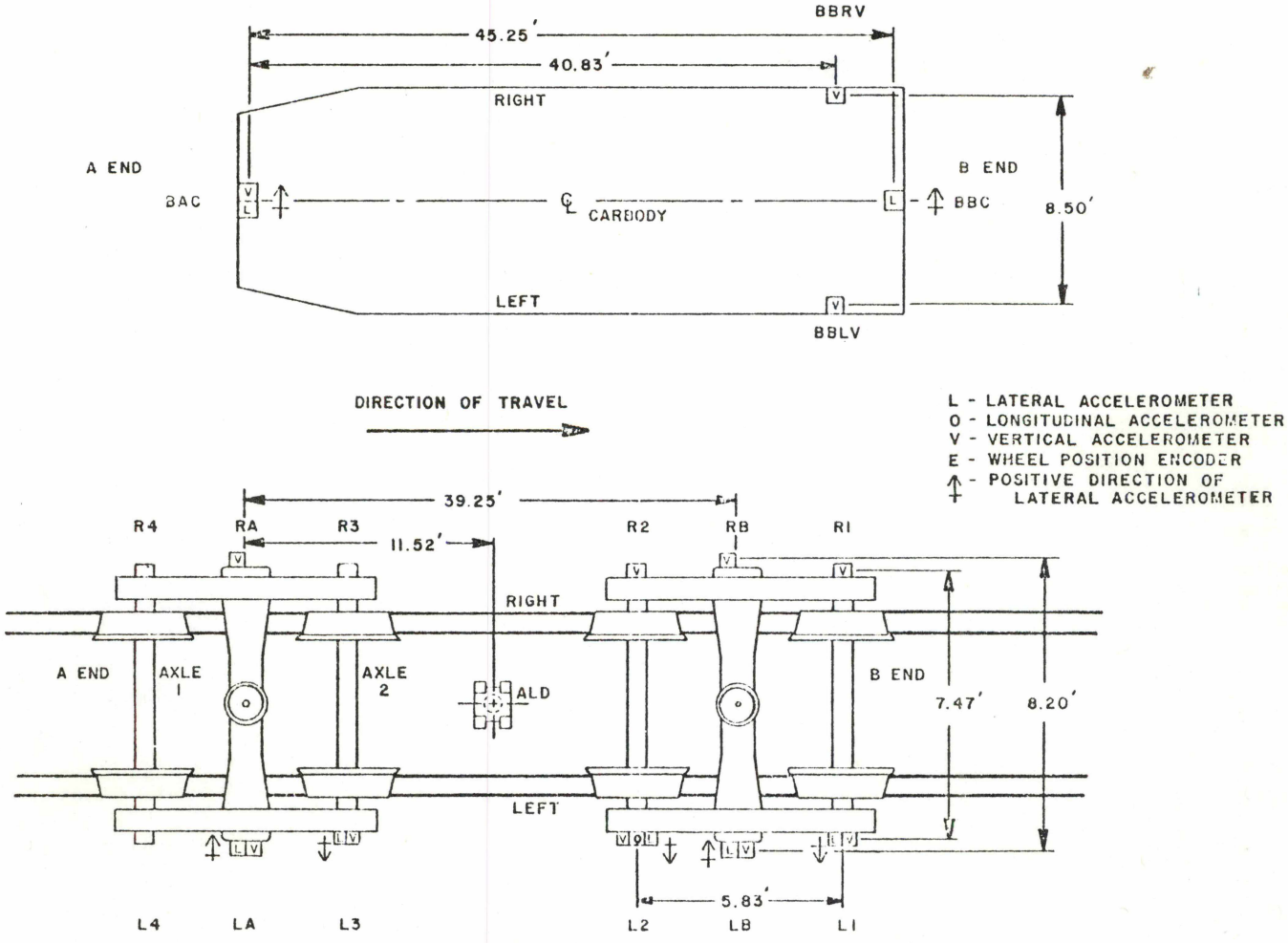

FIGURE 2-9. VECHICLE COMPONENT CONVENTIONS FOR CAR 46.

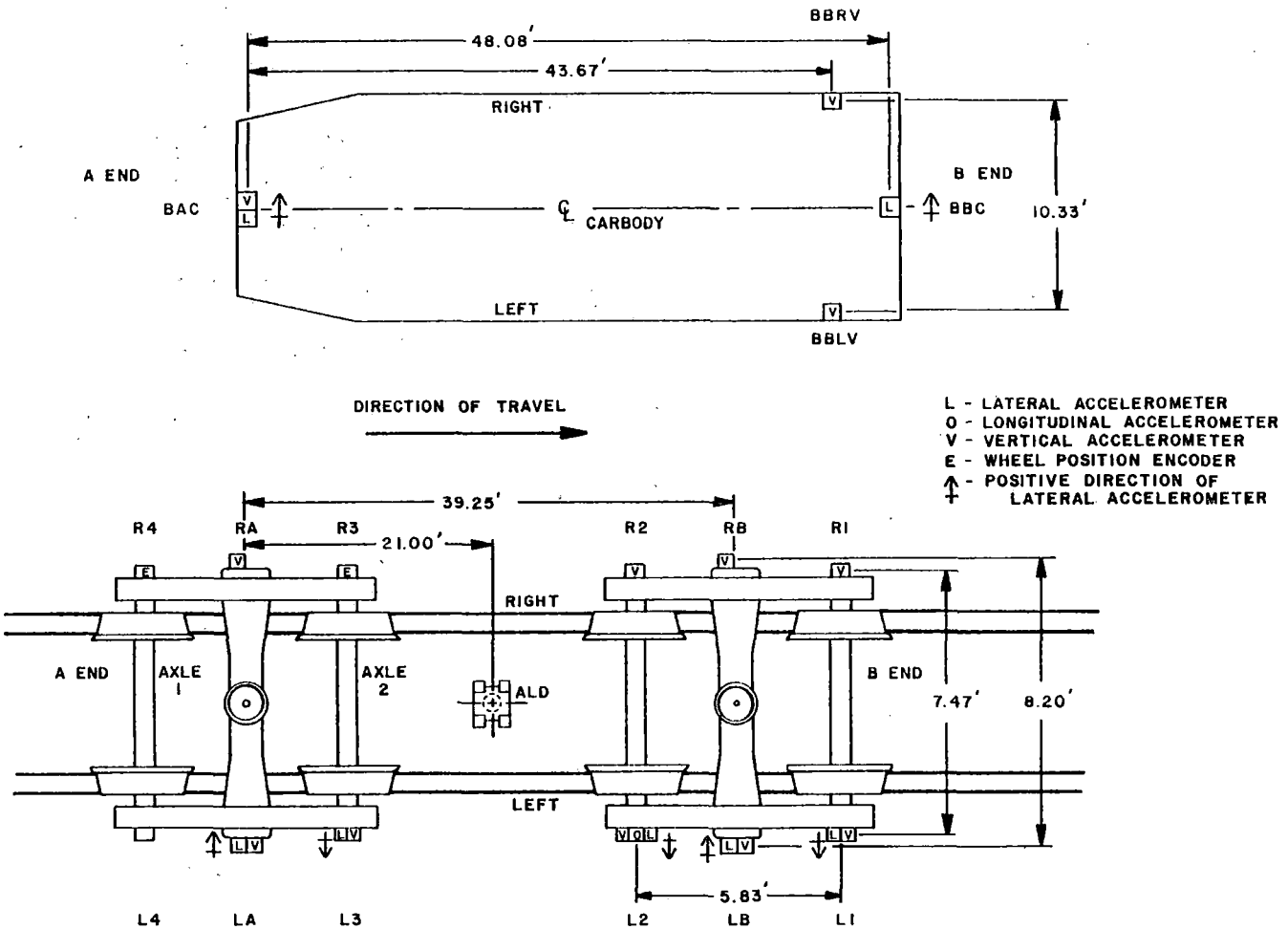

FIGURE 2-10. VECHICLE COMPONENT CONVENTIONS FOR CAR 47.

3.0 TEST PROCEDURES

3.1 GENERAL

Testing was conducted by assembling a special three-car test consist (figure 3-1) with a locomotive. All instrumentation was installed and tested prior to moving the consist to the test zones.

FIGURE 3-1. TYPICAL TEST CONSIST.

The test consist was first moved to Section 10 for calibration. This is a tangent section, which eliminated curvature and superelevation effects during calibration. After calibration, two clockwise runs around the FAST loop were made at constant speeds of 30 and 40 mi/h. Data were recorded for each run with the digital data acquisition system. The 40-mi/h run was terminated because there was excessive vibration from rail corrugations in Section 17. Therefore, data for this speed were not processed.

After completing the runs on the FAST loop, the consist was moved to the test zone on the RTT. Five passes over the RTT at speeds ranging from 10 to 50 mi/h in 10-mi/h increments were made in one direction, north to south. Data were collected during each pass. At the completion of the FAST and RTT tests, the instrumentation was transferred from one test vehicle to the other, except for the instrumented wheelset. The revised test consist then repeated the same RTT and FAST test series. At the completion of the test runs, the digital data tapes were regenerated in analog form to verify proper data recording and then shipped to ENSCO's facility for processing and storage. All testing was completed on February 25 and 26, 1977.

3.2 TEST CONSISTS

Two test consists were used because instrumentation was shared. Testing was performed on car 47 first and then on car 46. The test consists are shown schematically in figure 3-2.

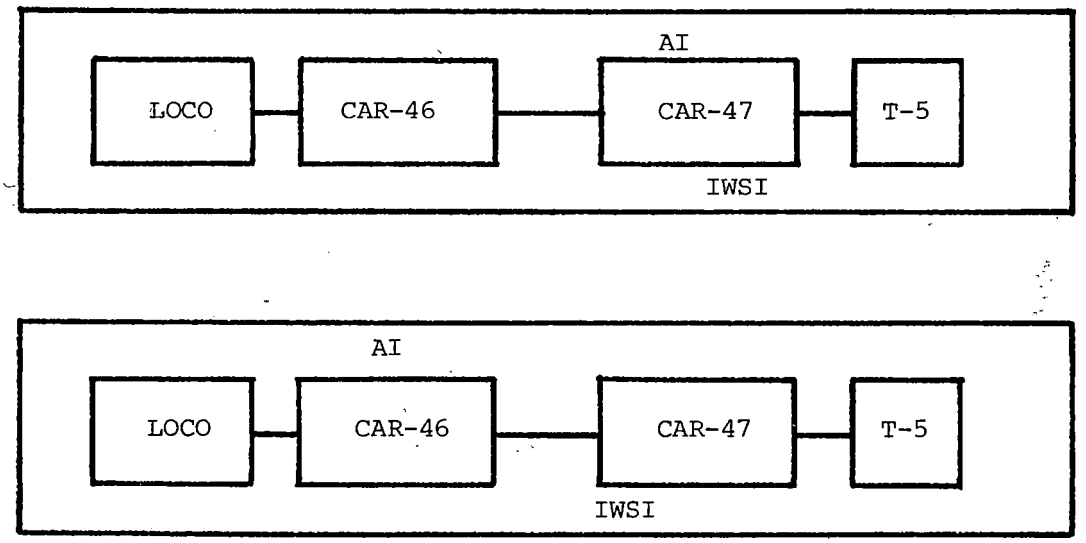

Note: AI - Accelerometers Installed
IWSI - Instrumented Wheelset Installed

FIGURE 3-2. CAR TEST CONSISTS.

4.0 TEST RESULTS

4.1 GENERAL

In this section the results of the third dynamic hopper car test are presented and discussed. The data were analyzed in terms of root mean square (rms) mode acceleration, wheel force, and transmissibility. A discussion of each of these techniques is given prior to the presentation of results.

Data collected on the FAST Track at a speed of 30 mi/h were analyzed in terms of RMS mode acceleration and wheel force. Discussions of these results are directed primarily at the effect of track structure on the ride performance of hopper cars. In addition, these data will be used to establish a baseline for comparative analysis with subsequent test results.

In the final subsection, the results of a transmissibility analysis are presented. Data for this analysis were obtained at five speeds (10, 20, 30, 40, and 50-mi/h) on the RTT. These results will be used to establish a similar baseline which will be used later to determine the effect of vehicle-component-wear on hopper car ride performance.

4.2 RMS MODE ACCELERATIONS

This study uses the modal representation for the accelerations of both the carbody and the trucks. This considers the motion of the carbody as being comprised of the six rigid-body degrees of freedom or modes. The modal representation of the trucks was similar, with the addition of a twist mode to account for the relative motion of truck components, basically the axles and side frames.

The mode accelerations were determined from acceleration data measured on the carbody and trucks. The requirements for sufficiency were that: (1) each measurementlocation be independent, and (2) there exist at least one measurement of acceleration for each mode to be determined. The calculation of carbody and truck modes is discussed in sections 4.2.1 and 4.2.2, respectively.

4.2.1 Carbody Mode Derivation

As outlined above, carbody accelerations were considered to be composed of six modes. Three of these modes were linear accelerations along the axes of a right-hand Cartesian coordinate system. The origin of this system was located at the geometric centroid of a horizontal planar section of the car. The remaining three modes were the angular accelerations about each of the three principle axes. The modes were referred to as longitudinal, lateral, bounce, roll, pitch, and yaw, denoted $\ddot{x}$, $\ddot{y}$, $\ddot{z}$, $\ddot{\theta}$, $\ddot{\phi}$, and $\ddot{\psi}$, respectively (figure 4-1). The double dot above each symbol denotes a double differentiation with respect to time (acceleration). Of the six modes given above, only five were determined. Longitudinal accelerations ($\ddot{x}$) were primarily influenced by train

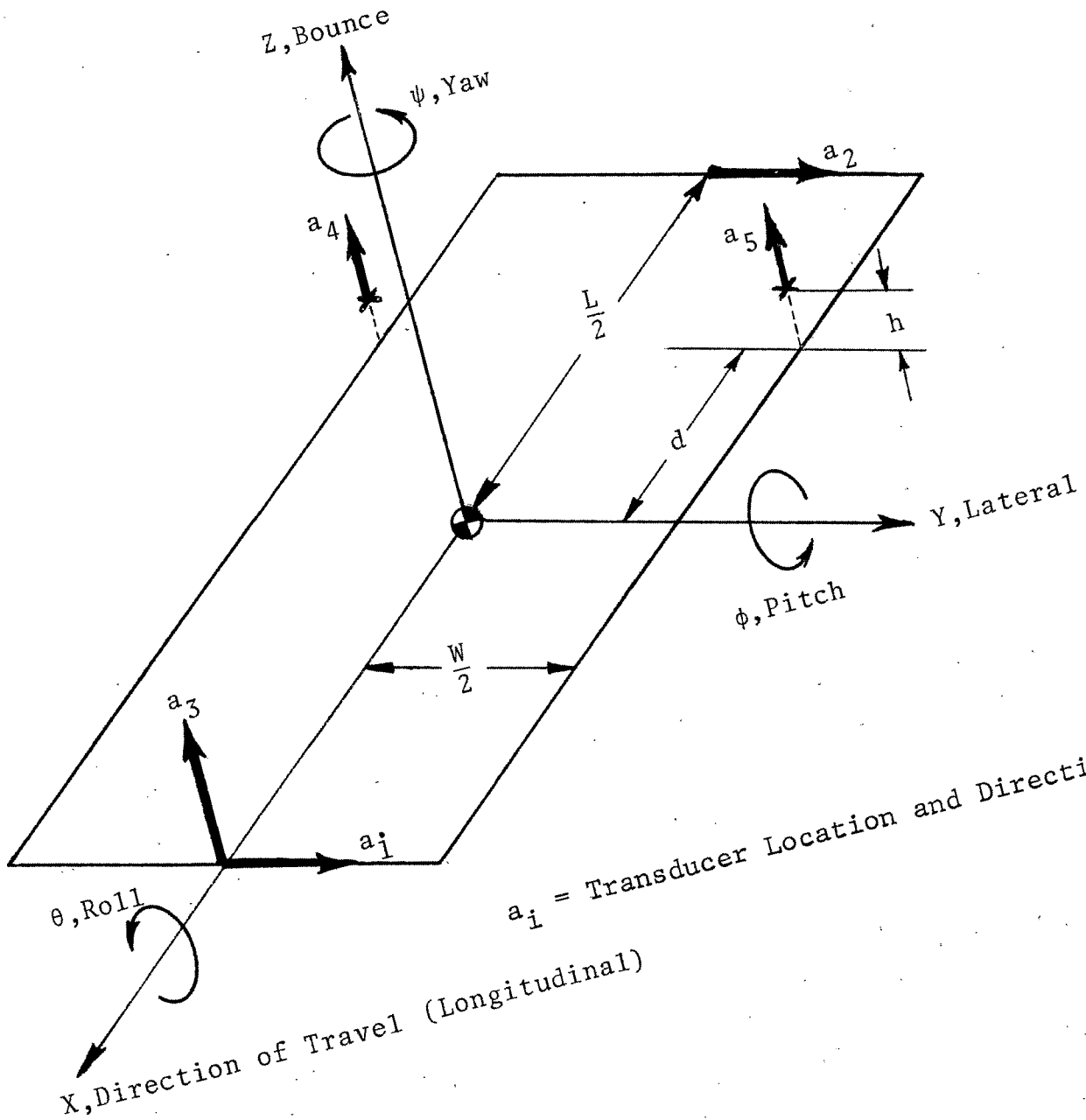

FIGURE 4-1. CARBODY CONVENTIONS AND TRANSDUCER LOCATIONS.

handling and were of lesser importance in this study. The remaining modes were to be determined by measurement of five accelerations indicated by bold face arrows labeled a_i (i=1, 2, 3, 4, and 5) in figure 4-1. Note that a_4 and a_5 lie a distance (h) above the plane of the other measurements. Writing these measurements in terms of their components yields:

$$a_1 = \ddot{y} + (L/2)\,\ddot{\psi}, \tag{1}$$

$$a_2 = \ddot{y} - (L/2)\,\ddot{\psi}, \tag{2}$$

$$a_3 = \ddot{z} - (L/2)\,\ddot{\phi}, \tag{3}$$

$$a_4 = \ddot{z} + d - (W/2)\,\ddot{\theta}, \tag{4}$$

$$a_5 = \ddot{z} + d + (W/2)\,\ddot{\theta}. \tag{5}$$

Making the following definition:

$$F = 2d + L\,,$$

and solving for the modes, one obtains:

$$\ddot{y} = (a_1 + a_2)/2\ , \tag{6}$$

$$\ddot{z} = \left[2da_3 + (L/2)(a_4 + a_5)\right]/F\ , \tag{7}$$

$$\ddot{\theta} = (a_5 - a_4)/W\ , \tag{8}$$

$$\ddot{\phi} = (a_4 + a_5 - 2a_3)/F\ , \tag{9}$$

$$\ddot{\psi} = (a_1 - a_2)/L\ . \tag{10}$$

Using these equations, the acceleration of each mode was calculated on a point-by-point basis in the time domain creating a mode acceleration time history. The mean or d.c. component was removed and the signal was low-pass-filtered at a corner frequency of 30 Hz. The result of this process was then used to calculate the rms acceleration of each mode.

4.2.2 Truck Mode Derivation

The definition and determination of truck modes were similar to that of the carbody with the addition of the twist mode. As before, a right-hand Cartesian coordinate system was used with its origin at the geometric centroid of the truck in the plane of the axles as shown in figure 4-2. These modes were directly analogous to those of the carbody and were given the same names and symbols. Figure 4-2 also shows the locations of the accelerations measured on the truck, a_i (i=1, 2, ... 6).

The trucks consist primarily of two axles and two side frames which behave as rigid bodies within the truck system. These subcomponents may displace angularly with respect to one another, resulting in a symmetrical twist mode as shown in figure 4-3. The twist angle (α) was taken about the x-axis and was measured in radians per unit length. Making the small angle approximation

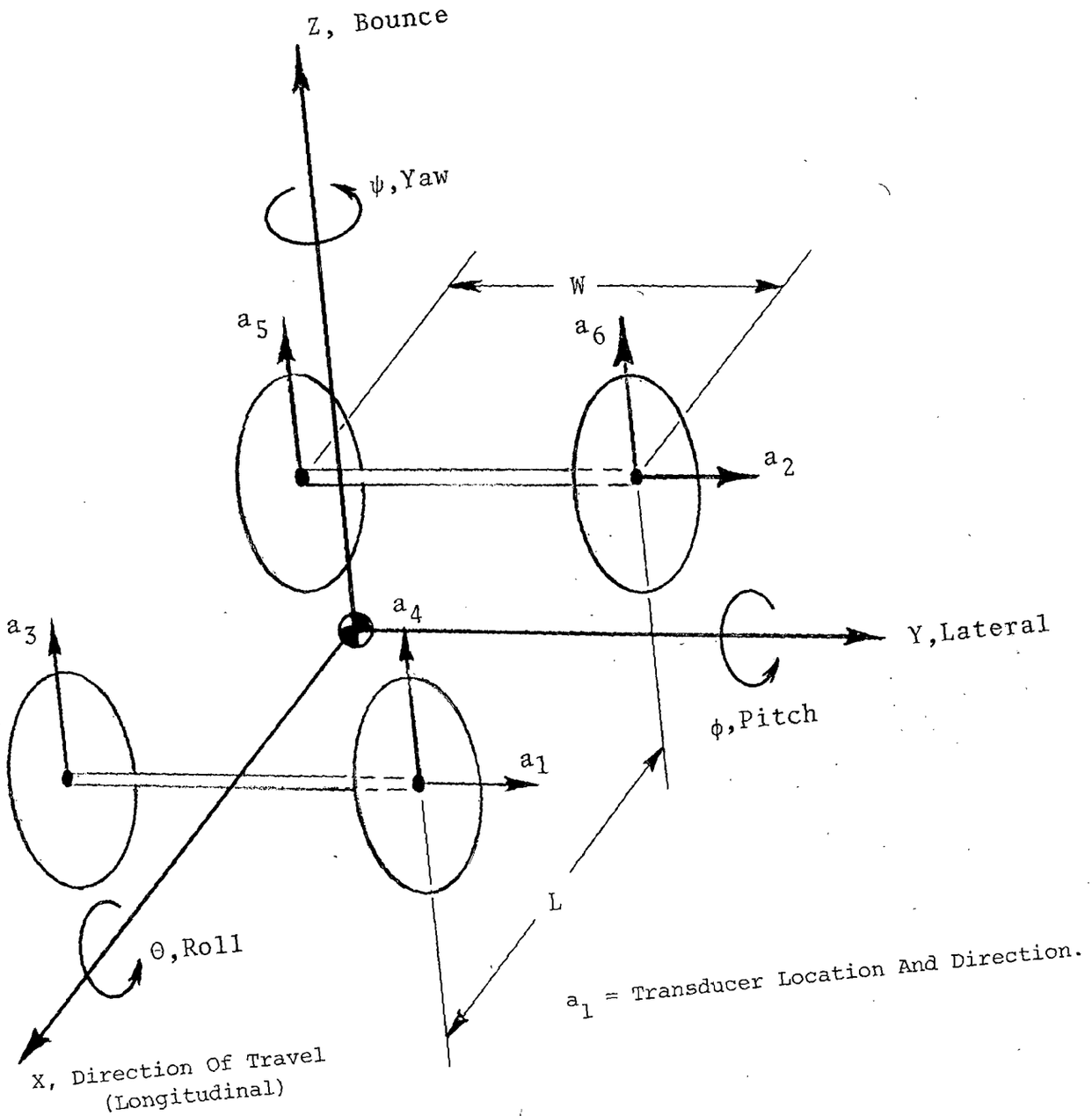

FIGURE 4-2. TRUCK CONVENTIONS AND TRANSDUCER LOCATIONS.

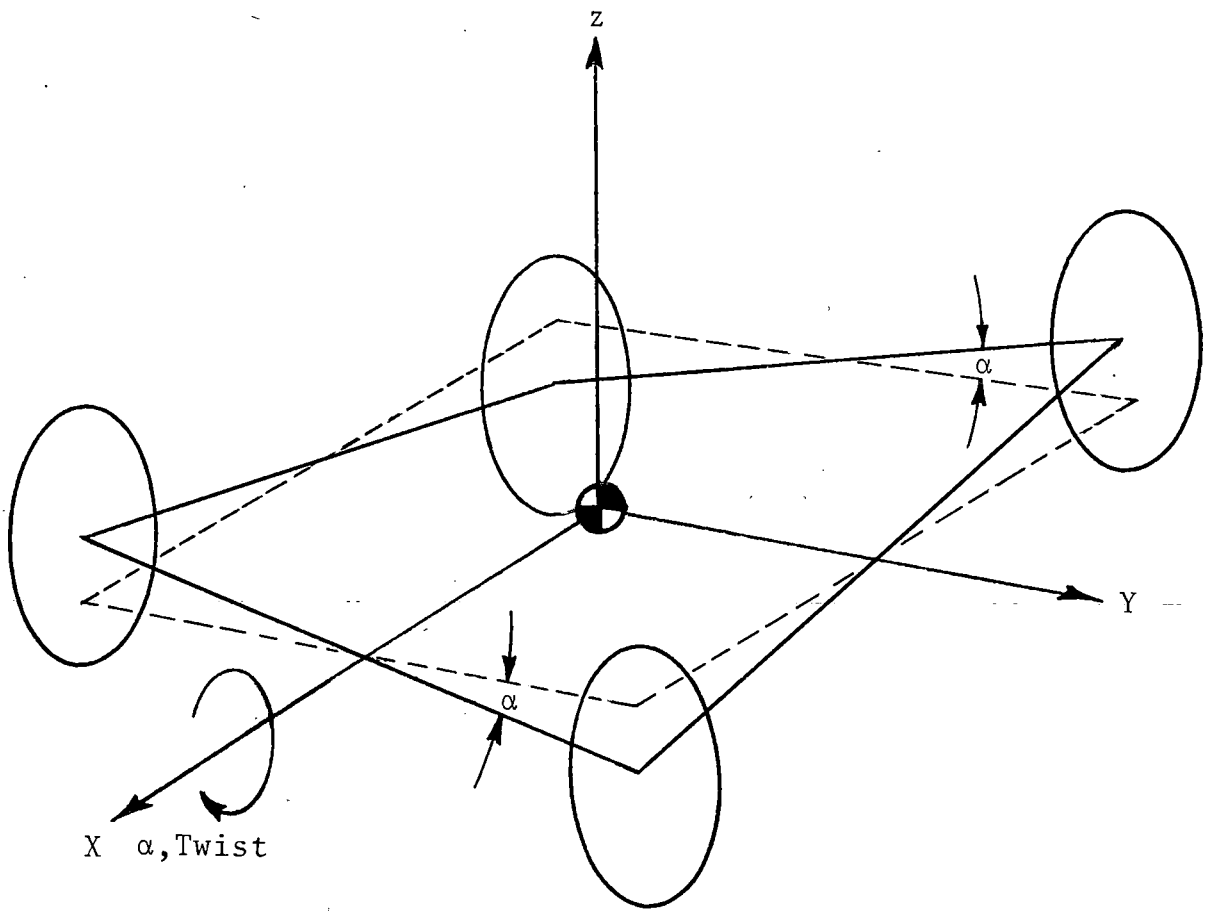

FIGURE 4-3. TRUCK TWIST MODE.

($\sin \alpha = \alpha$) and noting that twist and roll have opposite sign conventions, the measured acceleratons were written in terms of truck modes as:

$$a_1 = \ddot{y} + (L/2)\ddot{\psi} , \tag{11}$$

$$a_2 = \ddot{y} - (L/2)\ddot{\psi} , \tag{12}$$

$$a_3 = \ddot{z} - (W/2)\ddot{\theta} - (L/2)\ddot{\phi} + (WL/4)\ddot{\alpha} , \tag{13}$$

$$a_4 = \ddot{z} + (W/2)\ddot{\theta} - (L/2)\ddot{\phi} - (WL/4)\ddot{\alpha} , \tag{14}$$

$$a_5 = \ddot{z} - (W/2)\ddot{\theta} + (L/2)\ddot{\phi} - (WL/4)\ddot{\alpha} , \tag{15}$$

$$a_6 = \ddot{z} + (W/2)\ddot{\theta} + (L/2)\ddot{\phi} + (WL/4)\ddot{\alpha} . \tag{16}$$

Note that the sign of the twist changed, passing from the positive x-axis to the negative x-axis.

This system of equations can be solved for the truck modes, yielding:

$$\ddot{y} = (a_1 + a_2)/2 , \tag{17}$$

$$\ddot{z} = (a_3 + a_4 + a_5 + a_6)/4 , \tag{18}$$

$$\ddot{\theta} = (a_6 - a_5 + a_4 - a_3)/2W , \tag{19}$$

$$\ddot{\phi} = (a_6 + a_5 - a_4 - a_3)/2L , \tag{20}$$

$$\ddot{\psi} = (a_1 - a_2)/L , \tag{21}$$

$$\ddot{\alpha} = (a_6 - a_5 - a_4 + a_3)/WL . \tag{22}$$

Based on equations (6) through (10) for the carbody and equations (17) through (22) for the truck, individual measured accelerations can be transformed into eleven mode acceleration time series. The mode acceleration time series were then processed using standard statistical techniques to provide rms value, 95- and 99-percentile levels, histograms, and probability densities. The rms values of the modes were derived for each of the 22 FAST test sections. This technique provided data which were used to quantify the effect of track and roadbed composition on the dynamic performance of the truck and the carbody. Data presented in this manner will also be used in future tests to determine the effects of track degradation on vehicle performance.

In order to assess the effect of component wear on the ride performance of freight vehicles, the transmissibility between truck and carbody modes was determined. The transmissibility can be thought of as a characteristic of the freight car system which is independent of the condition of track over which the car is operated. Changes in transmissibility characteristics with accumulated mileage can therefore be directly attributed to changes in car components.

The transmissibility was formed in the frequency domain using PSD's. The mode acceleration time series were first transformed to a Fourier representation via a Fast Fourier Transform. Then the PSD of a given mode acceleration was generated by multiplication of the Fourier Transform with its complex conjugate. The power associated with each frequency increment of a selected carbody mode was then divided by the power associated with the corresponding frequency increment of a selected truck mode. The result is the spectral distribution of the mean square gain between the two selected modes.

The primary parameter used in the analysis of wheel force data is the lateral-to-vertical force ratio or L/V ratio. This ratio is an important safety index used to determine the potential of rail rollover and wheel flange climb. As discussed previously, lateral wheel forces were measured and recorded continuously, while vertical forces were measured accurately only four times per revolution. In order to construct a continuous L/V time series, the four vertical measurements were averaged over each wheel revolution. The continuous lateral force time series were then divided by the average vertical force for each wheel revolution. Statistical processing similar to that used for the acceleration modes provided L/V ratio and lateral wheel forces as a function of track sections.

4.2.3 Truck Mode Results

Truck mode accelerations for hopper cars 46 and 47 are plotted versus track section in figures 4-4 through 4-9. In addition, a statistical summary of the results is presented in table 4-1. A synopsis of a qualitative analysis is given in table 4-2 along with a brief description of each of the test sections.

Before discussing the results contained in table 4-2, a general observation concerning the comparison between the mode accelerations produced by the ASF truck (car 47) and those produced by the Barber S-2 truck (car 46) is in order. From figures 4-4 through 4-9, it can be seen that the magnitude of the rms mode accelerations for each truck were in general the same. This result was anticipated since the mode accelerations of the truck are only a function of truck dimensions, track geometry, and speed. Since data were acquired at the same speed over the same track and the dimensions of each truck were nearly identical, the results were anticipated. This was not the case, however, for the carbody modes since the suspension elements of the truck play a major part in determining the magnitude of these modes.

The qualitative analysis of table 4-2 classifies the relative levels of mode acceleration for each test section as either high, moderate, or low. Significant events which had an appreciable influence on this rating and were observed in the time histories are also noted. Based on this information, the following conclusions were drawn.

Those test sections which exhibited high levels of accelerations contained curves (greater than 4°), frogs, guard rails, and turnouts. In most modes, Section 11 produced the highest levels of acceleration and it contained guard rails, frogs, and staggered joints. Sections 01, 16, and 21 were short sections containing a single turnout; rms acceleration levels in these

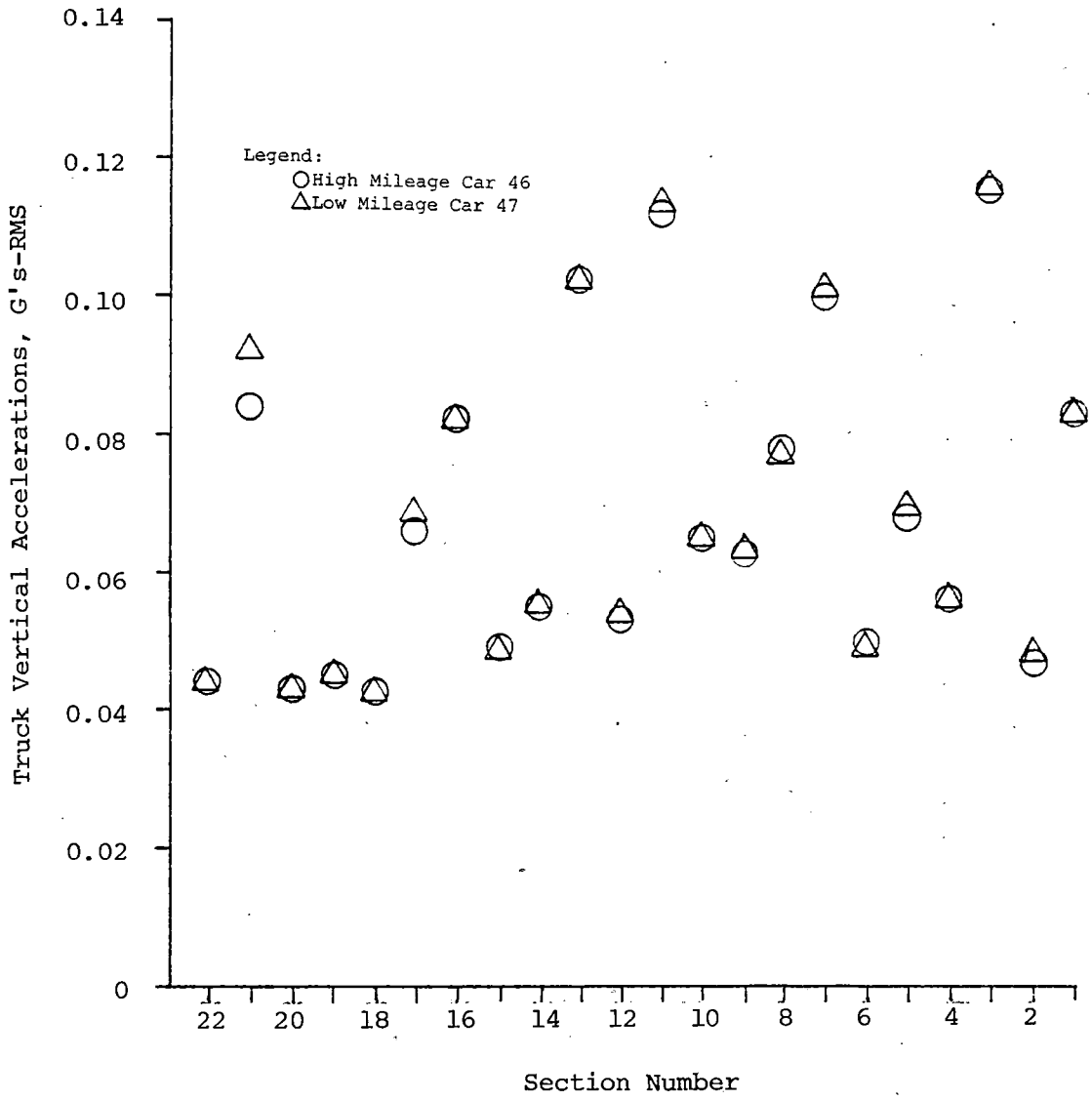

FIGURE 4-4. TRUCK VERTICAL ACCELERATIONS VS. SECTION.

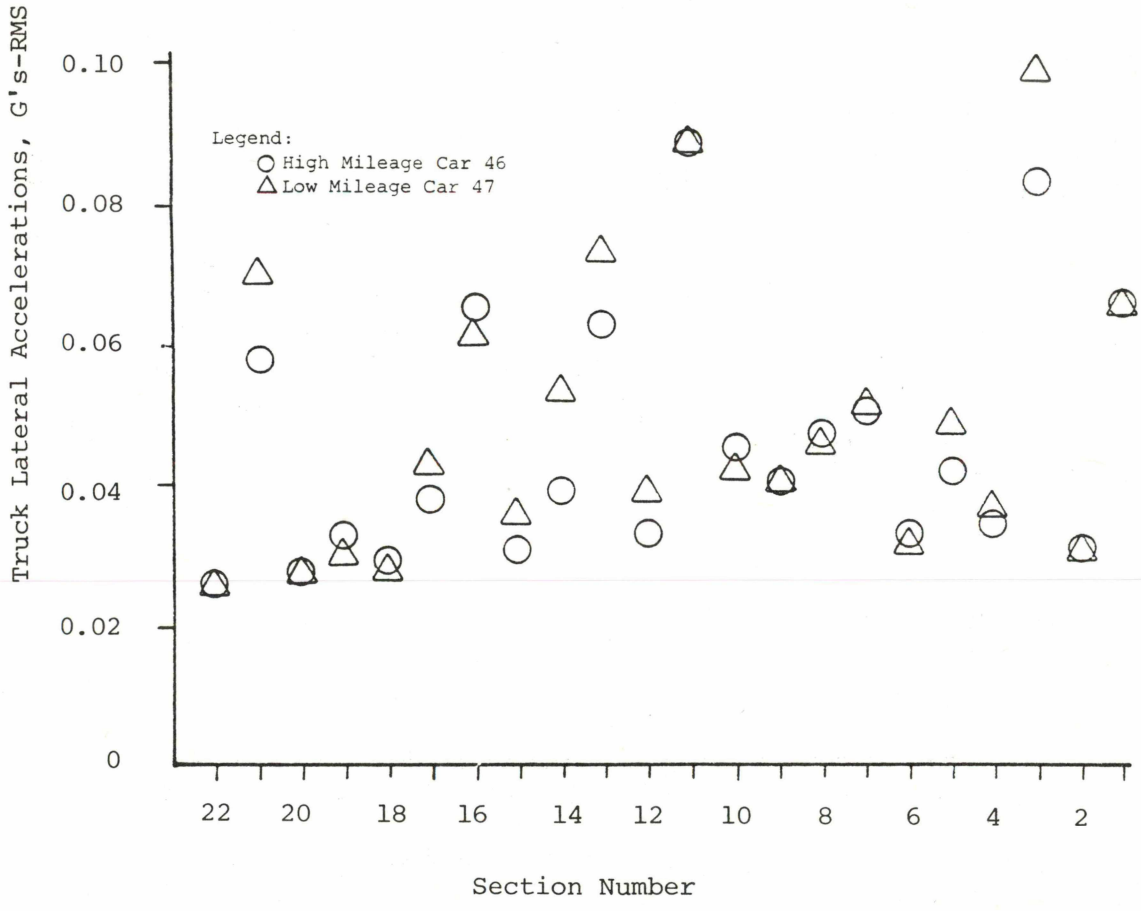

FIGURE 4-5. TRUCK LATERAL ACCELERATIONS VS. SECTION.

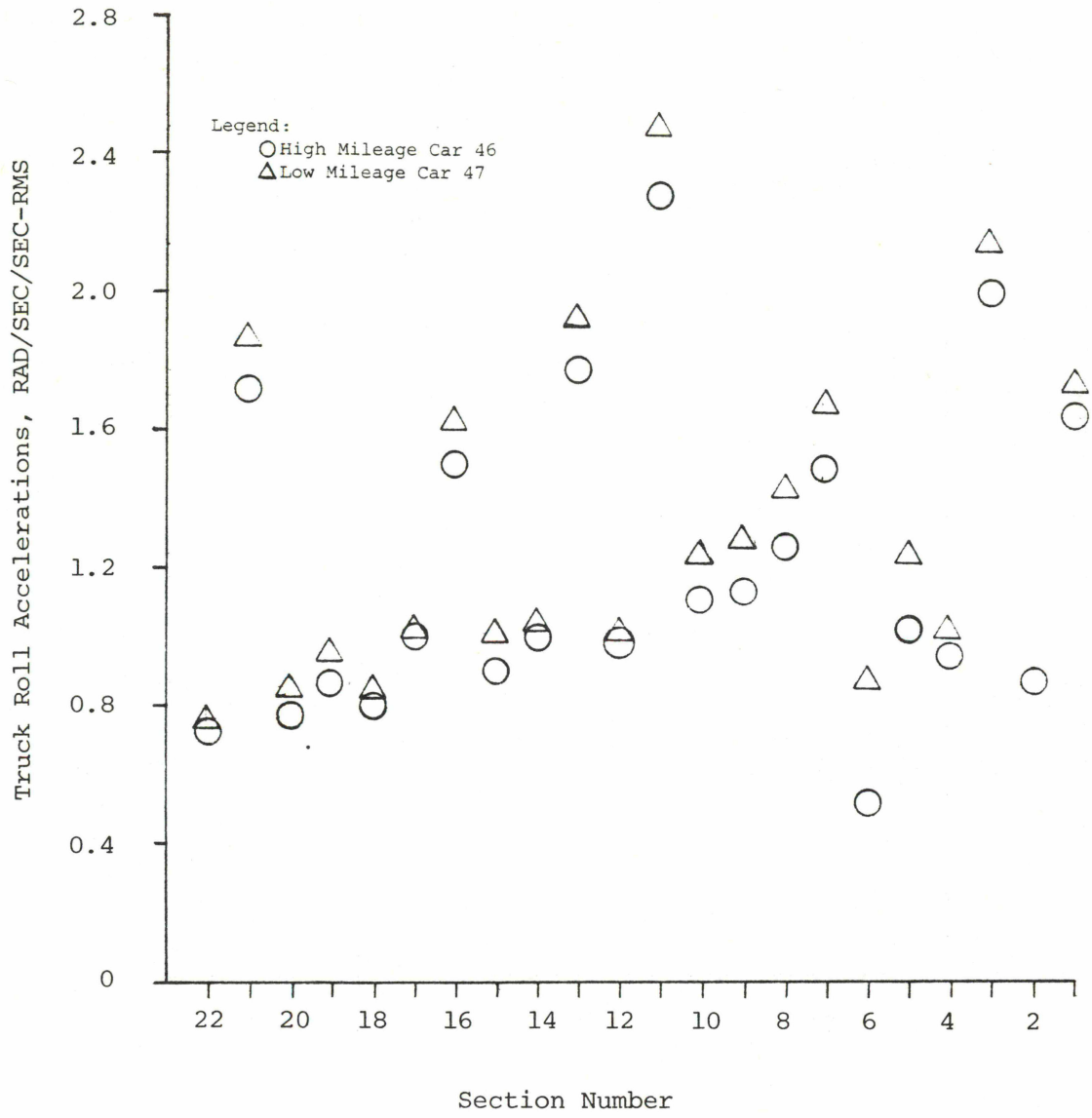

FIGURE 4-6. TRUCK ROLL ACCELERATIONS VS. SECTION.

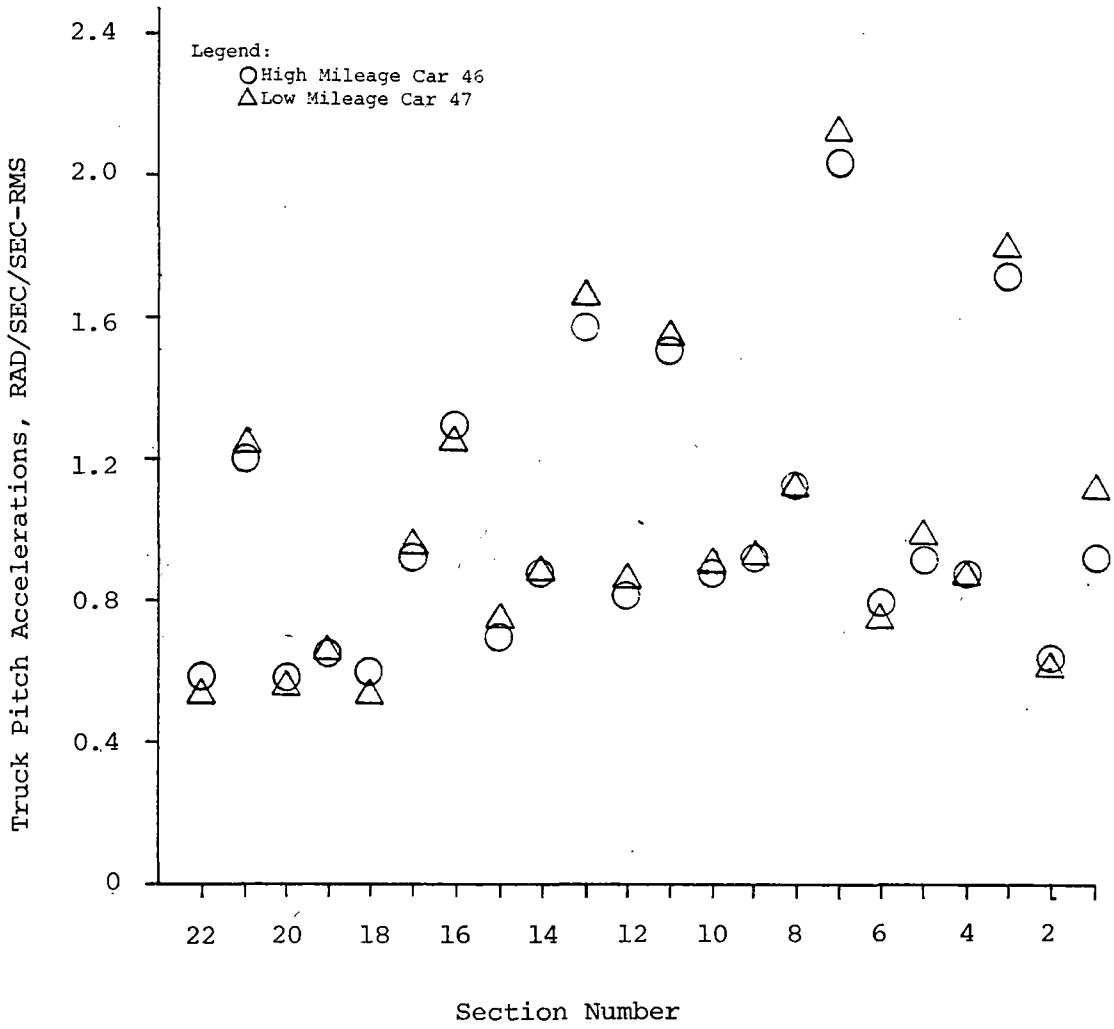

FIGURE 4-7. TRUCK PITCH ACCELERATIONS VS. SECTION.

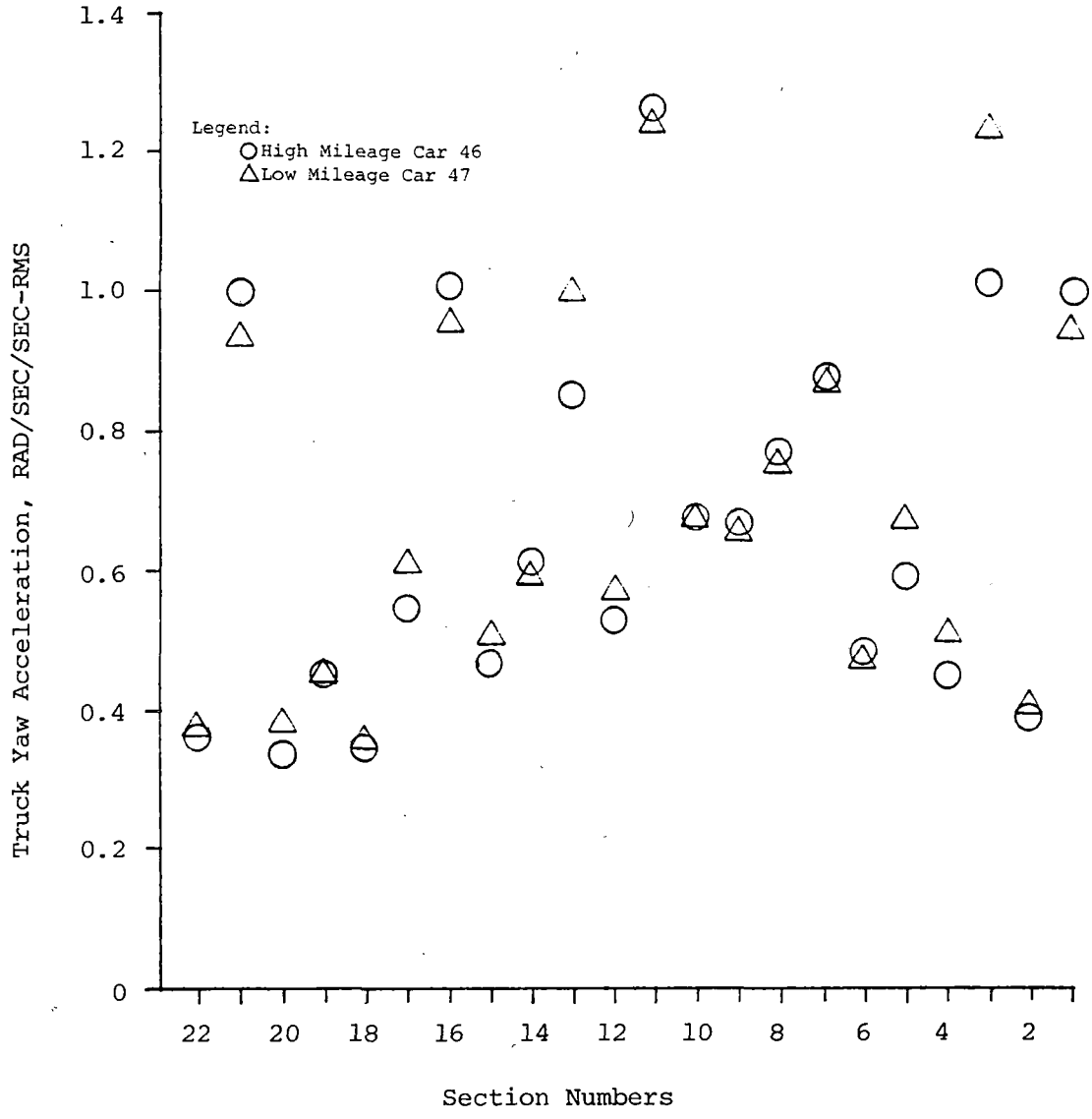

FIGURE 4-8. TRUCK YAW ACCELERATIONS VS. SECTION.

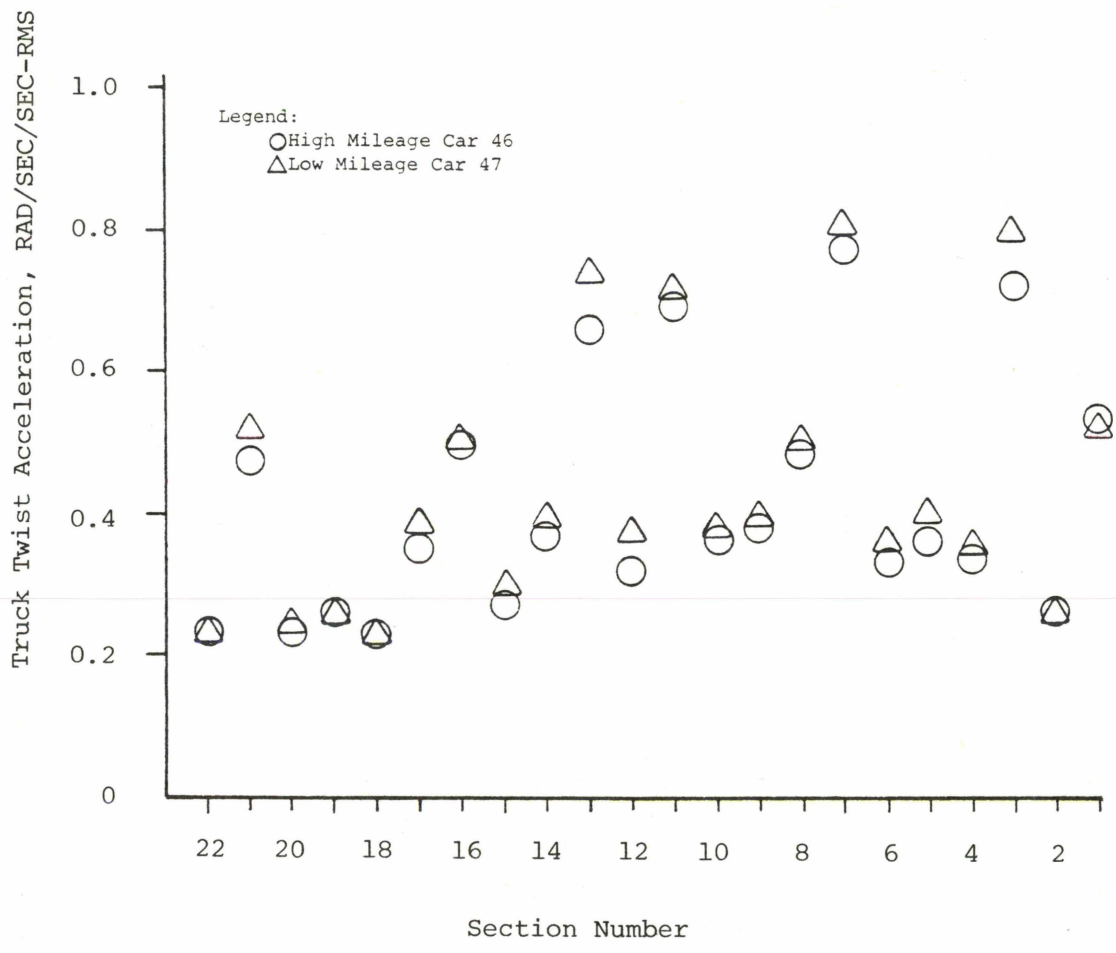

FIGURE 4-9. TRUCK TWIST ACCELERATIONS VS. SECTION.

TABLE 4-1. TRUCK ACCELERATION STATISTICS.

	TRUCK											
	46	47	46	47	46	47	46	47	46	47	46	47
Section	G's Vertical		G's Lateral		Rad/Sec^2 Roll		Rad/Sec^2 Pitch		Rad/Sec^2 Yaw		Rad/Sec^2 Twist	
01												
St Dev	0.09	0.09	0.07	0.07	1.74	1.77	1.24	1.16	1.14	1.04	0.58	0.56
95%	0.17	0.18	0.15	0.15	3.20	3.56	2.65	2.43	2.05	2.15	1.20	1.22
99%	0.38	0.37	0.33	0.33	8.21	8.19	5.39	4.93	4.82	4.81	2.52	2.47
RMS	0.08	0.08	0.07	0.07	1.63	1.68	1.23	1.10	1.00	0.95	0.53	0.52
02												
St Dev	0.05	0.04	0.03	0.03	0.93	0.91	0.68	0.62	0.42	0.44	0.28	0.29
95%	0.09	0.08	0.06	0.06	1.63	1.61	1.25	1.21	0.80	0.87	0.55	0.56
99%	0.14	0.14	0.09	0.09	2.96	3.17	2.11	2.27	1.31	1.52	0.90	1.01
RMS	0.05	0.04	0.03	0.03	0.86	0.83	0.65	0.60	0.39	0.41	0.26	0.26
03												
St Dev	0.12	0.13	0.09	0.11	2.15	2.29	1.86	1.96	1.16	1.35	0.78	0.87
95%	0.26	0.27	0.19	0.23	4.42	4.75	3.91	4.18	2.38	2.81	1.69	1.89
99%	0.45	0.47	0.33	0.40	8.49	8.76	7.16	7.44	4.27	4.98	2.89	3.13
RMS	0.12	0.12	0.08	0.10	1.99	2.13	1.71	1.80	1.06	1.23	0.72	0.80
04												
St Dev	0.06	0.06	0.04	0.04	0.99	1.09	0.99	0.98	0.48	0.53	0.37	0.39
95%	0.12	0.12	0.07	0.08	2.12	2.30	2.16	2.07	1.01	1.08	0.81	0.80
99%	0.18	0.24	0.10	0.13	2.85	3.61	3.09	3.60	1.45	1.56	1.13	1.20
RMS	0.06	0.05	0.03	0.00	0.94	1.01	0.87	0.85	0.44	0.51	0.33	0.35

TABLE 4-1. TRUCK ACCELERATION STATISTICS, CONTINUED.

	TRUCK											
	46	47	46	47	46	47	46	47	46	47	46	47
Section	G's Vertical		G's Lateral		Rad/Sec^2 Roll		Rad/Sec^2 Pitch		Rad/Sec^2 Yaw		Rad/Sec^2 Twist	
05												
St Dev	0.59	0.08	0.04	0.05	0.97	1.33	0.85	1.04	0.57	0.75	0.33	0.43
95%	0.12	0.12	0.08	0.09	1.84	2.22	1.60	1.69	1.07	1.42	0.64	0.69
99%	0.18	0.26	0.13	0.20	2.70	6.36	2.75	5.64	1.83	3.42	0.99	2.07
RMS	0.07	0.07	0.04	0.05	1.08	1.25	0.91	0.10	0.60	0.69	0.36	0.40
06												
St Dev	0.06	0.05	0.04	0.03	1.12	0.93	0.88	0.76	0.56	0.48	0.37	0.32
95%	0.10	0.09	0.07	0.06	1.88	1.73	1.47	1.45	1.03	0.93	0.62	0.64
99%	0.20	0.17	0.12	0.10	3.90	3.48	3.28	2.73	1.89	0.50	1.20	1.03
RMS	0.05	0.05	0.03	0.03	0.91	0.86	0.79	0.78	0.49	0.47	0.33	0.36
07												
St Dev	0.10	0.11	0.05	0.05	1.53	1.73	2.10	2.20	0.91	0.90	0.80	0.84
95%	0.21	0.22	0.10	0.10	3.03	3.49	4.29	4.48	1.77	1.73	1.64	1.68
99%	0.31	0.35	0.15	0.16	4.75	5.16	6.25	6.38	2.71	2.64	2.43	2.67
RMS	0.10	0.10	0.05	0.05	1.47	1.66	2.05	2.15	0.88	0.86	0.77	0.81
08												
St Dev	0.08	0.08	0.05	0.05	1.30	1.48	1.25	1.27	0.80	0.81	0.51	0.53
95%	0.16	0.17	0.09	0.09	2.61	3.04	2.88	2.90	1.51	1.51	1.08	1.13
99%	0.30	0.32	0.18	0.16	4.91	5.83	4.73	4.86	2.63	3.02	1.73	2.00
RMS	0.08	0.08	0.05	0.05	1.26	1.44	1.14	1.14	0.77	0.74	0.48	0.50

TABLE 4-1. TRUCK ACCELERATION STATISTICS, CONTINUED.

	TRUCK											
	46	47	46	47	46	47	46	47	46	47	46	47
Section	G's Vertical		G's Lateral		Rad/Sec^2 Roll		Rad/Sec^2 Pitch		Rad/Sec^2 Yaw		Rad/Sec^2 Twist	
09												
St Dev	0.07	0.07	0.04	0.05	1.22	1.37	0.99	1.00	0.80	0.73	0.42	0.44
95%	0.13	0.14	0.09	0.08	2.42	2.67	1.88	1.87	1.41	1.46	0.84	0.86
99%	0.26	0.30	0.16	0.20	4.60	5.72	4.01	4.22	3.48	2.79	1.54	1.82
RMS	0.06	0.07	0.04	0.04	1.12	1.24	0.96	0.93	0.68	0.65	0.38	0.40
10												
St Dev	0.07	0.07	0.06	0.05	1.26	1.39	0.96	0.99	0.82	0.79	0.41	0.43
95%	0.13	0.13	0.09	0.09	2.36	2.72	1.79	1.85	1.59	1.51	0.78	0.83
99%	0.29	0.31	0.21	0.21	5.16	5.90	4.02	4.24	3.19	3.17	1.80	1.96
RMS	0.07	0.07	0.05	0.04	1.11	1.22	0.88	0.90	0.68	0.67	0.36	0.38
11												
St Dev	0.12	0.13	0.10	0.10	2.52	2.72	1.63	1.68	1.39	1.38	0.77	0.78
95%	0.25	0.27	0.20	0.20	5.49	6.28	3.43	3.43	2.88	2.80	1.56	1.67
99%	0.55	0.57	0.45	0.46	11.27	11.74	7.26	7.29	5.85	5.97	3.44	3.50
RMS	0.11	0.12	0.09	0.09	2.28	2.48	1.51	1.54	1.26	1.26	0.70	0.72
12												
St Dev	0.05	0.06	0.03	0.04	0.98	1.03	0.81	0.87	0.53	0.58	0.32	0.37
95%	0.11	0.11	0.07	0.07	1.94	1.99	1.58	1.66	0.98	1.03	0.60	0.69
99%	0.16	0.19	0.09	0.11	3.21	3.71	2.57	2.91	1.75	1.97	0.99	1.22
RMS	0.05	0.06	0.03	0.04	0.98	1.05	0.82	0.86	0.53	0.58	0.32	0.37

TABLE 4-1. TRUCK ACCELERATION STATISTICS, CONTINUED.

	TRUCK											
	46	47	46	47	46	47	46	47	46	47	46	47
Section	G's Vertical		G's Lateral		Rad/Sec^2 Roll		Rad/Sec^2 Pitch		Rad/Sec^2 Yaw		Rad/Sec^2 Twist	
13												
St Dev	0.11	0.11	0.07	0.08	1.83	2.01	1.61	1.73	0.89	1.03	0.68	0.77
95%	0.21	0.23	0.13	0.15	3.85	4.31	3.40	3.66	1.83	2.09	1.43	1.65
99%	0.41	0.38	0.23	0.28	7.12	7.83	5.83	6.52	3.29	3.72	2.38	2.64
RMS	0.10	0.10	0.06	0.07	1.77	1.93	1.55	1.66	0.85	1.00	0.66	0.74
14												
St Dev	0.06	0.06	0.05	0.05	1.18	1.26	1.01	1.00	0.72	0.67	0.42	0.44
95%	0.11	0.12	0.08	0.09	2.25	2.40	2.05	2.05	1.29	1.33	0.87	0.90
99%	0.22	0.23	0.15	0.17	4.19	4.91	3.38	3.51	2.60	2.43	1.68	1.69
RMS	0.06	0.06	0.04	0.04	1.05	1.12	0.88	0.89	0.62	0.60	0.37	0.38
15												
St Dev	0.05	0.05	0.03	0.03	0.90	1.00	0.70	0.74	0.47	0.49	0.28	0.30
95%	0.09	0.10	0.06	0.07	1.80	2.00	1.37	1.47	0.94	0.99	0.55	0.61
99%	0.15	0.15	0.09	0.11	2.69	3.13	2.16	2.37	1.40	1.45	0.79	0.99
RMS	0.05	0.05	0.03	0.04	0.90	1.00	0.70	0.75	0.47	0.51	0.28	0.30
16												
St Dev	0.09	0.09	0.07	0.07	1.66	1.88	1.40	1.46	1.16	1.18	0.54	0.59
95%	0.16	0.18	0.14	0.14	3.28	3.86	2.98	3.01	2.05	2.21	1.09	1.19
99%	0.36	0.39	0.31	0.29	7.01	7.07	4.76	5.39	5.69	4.77	2.22	2.32
RMS	0.08	0.08	0.07	0.06	1.51	1.63	1.28	1.25	1.02	0.96	0.50	0.51

TABLE 4-1. TRUCK ACCELERATION STATISTICS, CONTINUED.

Section	TRUCK											
	46	47	46	47	46	47	46	47	46	47	46	47
	G's Vertical		G's Lateral		Rad/Sec^2 Roll		Rad/Sec^2 Pitch		Rad/Sec^2 Yaw		Rad/Sec^2 Twist	
17												
St Dev	0.75	0.08	0.04	0.49	1.13	1.26	1.12	1.22	0.61	0.67	0.42	0.47
95%	0.15	0.17	0.09	0.10	2.34	2.64	2.38	2.62	1.28	1.39	0.89	1.00
99%	0.27	0.30	0.15	0.16	4.10	4.55	4.42	5.00	2.17	2.28	1.65	1.91
RMS	0.07	0.07	0.04	0.04	1.02	1.12	0.93	0.98	0.55	0.61	0.35	0.39
18												
St Dev	0.05	0.05	0.03	0.03	0.82	0.88	0.61	0.60	0.36	0.39	0.24	0.25
95%	0.09	0.09	0.06	0.06	1.59	1.71	1.17	1.16	0.72	0.74	0.45	0.47
99%	0.13	0.16	0.09	0.09	2.45	2.91	1.77	1.94	1.08	1.27	0.76	0.79
RMS	0.04	0.04	0.03	0.03	0.80	0.84	0.59	0.57	0.34	0.36	0.23	0.24
19												
St Dev	0.05	0.05	0.03	0.03	0.89	0.99	0.67	0.67	0.46	0.45	0.27	0.27
95%	0.09	0.09	0.07	0.06	1.67	1.73	1.29	1.26	0.91	0.89	0.53	0.53
99%	0.15	0.15	0.11	0.09	3.17	3.38	2.28	2.27	1.55	1.57	0.87	0.96
RMS	0.05	0.05	0.03	0.03	0.87	0.95	0.65	0.66	0.45	0.45	0.26	0.27
20												
St Dev	0.04	0.04	0.03	0.03	0.79	0.85	0.58	0.58	0.34	0.38	0.23	0.25
95%	0.08	0.08	0.05	0.06	1.57	1.68	1.14	1.14	0.69	0.76	0.46	0.48
99%	0.12	0.13	0.08	0.08	2.31	2.57	1.66	1.74	0.96	1.05	0.69	0.75
RMS	0.04	0.04	0.03	0.03	0.78	0.85	0.58	0.58	0.35	0.38	0.23	0.25

TABLE 4-1. TRUCK ACCELERATION STATISTICS, CONTINUED.

	TRUCK											
	46	47	46	47	46	47	46	47	46	47	46	47
Section	G's Vertical		G's Lateral		Rad/Sec^2 Roll		Rad/Sec^2 Pitch		Rad/Sec^2 Yaw		Rad/Sec^2 Twist	
21												
St Dev	0.09	0.10	0.06	0.07	1.85	2.17	1.26	1.39	1.12	0.92	0.51	0.59
95%	0.20	0.21	0.12	0.14	4.11	4.50	2.66	3.20	1.65	1.80	1.17	1.31
99%	0.32	0.42	0.22	0.33	6.74	9.53	4.28	5.77	4.45	3.75	1.74	2.23
RMS	0.08	0.09	0.06	0.07	1.67	1.87	1.20	1.24	1.00	0.93	0.48	0.52
22												
St Dev	0.05	0.05	0.03	0.03	0.78	0.82	0.62	0.59	0.41	0.44	0.24	0.25
95%	0.09	0.09	0.06	0.06	1.48	1.57	1.19	1.12	0.75	0.78	0.46	0.47
99%	0.14	0.14	0.09	0.10	2.38	2.69	2.04	2.08	1.34	1.43	0.79	0.80
RMS	0.04	0.04	0.03	0.03	0.74	0.76	0.58	0.55	0.37	0.38	0.23	0.23

TABLE 4-2. TRACK AND TRUCK ACCELERATION SUMMARY.

Section	Length (ft)	Description	Comments On Track	Relative Acceleration Level
01	170	Spiral	Turnout	High
02	329	Spiral	Rubber pads (one of lowest)	Low
03	3,740	5° Curve	Spliced short length rail (Highest vertical)	High
04	310	Spiral	Standard CWR	Low
05	222	Tangent	Bonded joints unsupported	Low
06	300	Spiral	Standard, CWR (Steel ties removed 1-04-77)	Low
07	1,000	5° Curve	Rail tie fasteners (Highest twist and pitch)	High
08	300	Spiral	Standard, CWR	Moderate
09	628	Tangent	Reconstituted & laminated wood ties, elastic spikes, safety equipment, turnouts	Moderate
10	1,550	Tangent	Spring frogs & guard rail	Moderate
11	895	Tangent	Joints, frogs & guard rail (Dominated by 8 discrete events)	High
12	339	Spiral & 4° Curve	Jointed rail	Moderate
13	1,248	4° Curve	Rail metallurgy & spike hole fillers, CWR	High
14	818	4° Curve & Spiral	Standard No. 20 turnout (Dominated by a single discrete event)	Low/Moderate
15	1,300	Tangent	Different ballast shoulder widths	Low
16	222	Tangent	Glued No. 20 turnout	High
17	6,143	Tangent, Spirals & Curves (3° and 5°	Concrete tie & tie pads	Low

TABLE 4-2. TRACK AND TRUCK ACCELERATION SUMMARY, CONTINUED.

Section	Length (ft)	Description	Comments On Track	Relative Acceleration Level
18	822	Tangent	Different ballast depths	Low
19	600	Spirals	Hardwood & softwood ties	Low
20	2,278	Tangent	Ballast types & depths; rail anchors	Low
21	172	Tangent	No. 20 welded turnout	High
22	1,950	Tangent	Spiking patterns & rail anchors	Low

sections were relatively high and in each case were dominated by the acceleration impulse experienced at the turnout.

Two other sections exhibited relatively large accelerations in limited portions of the data. Section 07 produced the highest pitch acceleration and high bounce and roll accelerations, but the lateral and yaw modes were relatively low. This section is 1,000 ft of 5° curve, which suppressed accelerations in the lateral and yaw modes. As the consist entered Section 17 (spiral-to-3° curve) from Section 18, all modes were excited at relatively low levels. However, on entering subsection 17D (5° curve), the levels of all modes increased dramatically. In particular, the pitch, yaw, and twist modes doubled in amplitude. Subsections D through A of Section 17 comprise a 1,300-ft, 5° curve which had heavy rail corrugations. This explains the high levels of acceleration observed.

In contrast to the sections discussed in the previous paragraphs, there were a large number of sections which produced relatively low levels of acceleration. These sections were generally tangent or spiral with both welded and jointed rail with combinations of rubber pads, different types of ties, ballast, rail anchors, and spiking patterns. However, no particular section of track produced an absolute lowest acceleration level for all modes. It was, therefore, concluded that variations in these track structure characteristics produced very little effect in truck mode accelerations.

Three sections were classified as moderate. These were Sections 08, 09, and 10. Two of these are tangent and one, Section 08, is a short spiral. Section 10 contained spring frogs, guard rails, and two turnouts. As a result, there were three distinct events in Section 10 which caused its moderate rating. Section 09 was dominated by a single distinct event.

4.2.4 Carbody Mode Results

The results of carbody mode acceleration calculations are presented in figures 4-10 through 4-14 along with a statistical summary in table 4-3. The first observation, based on these figures, was that significant differences existed between carbody modes on hopper cars 46 and 47. This probably is due to the fact that the suspension elements on each car were different. The following observations are in order.

In the lateral mode, the low-mileage or control car (No. 47) experienced lower levels of acceleration in 10 of the 22 sections, while car 46 experienced lower levels in only six sections. In the remaining six sections, the lateral acceleration levels were approximately the same. Thus, it was concluded that the lateral suspension characteristics of the car 47 were marginally better than those of the car 46.

The situation was somewhat reversed in the vertical mode with car 46 showing lower accelerations in six sections compared to only three sections for car 47. In the remaining 13 sections, the performance of the two cars was very nearly the same and no definite conclusion could be reached concerning relative merits of the cars in the vertical mode.

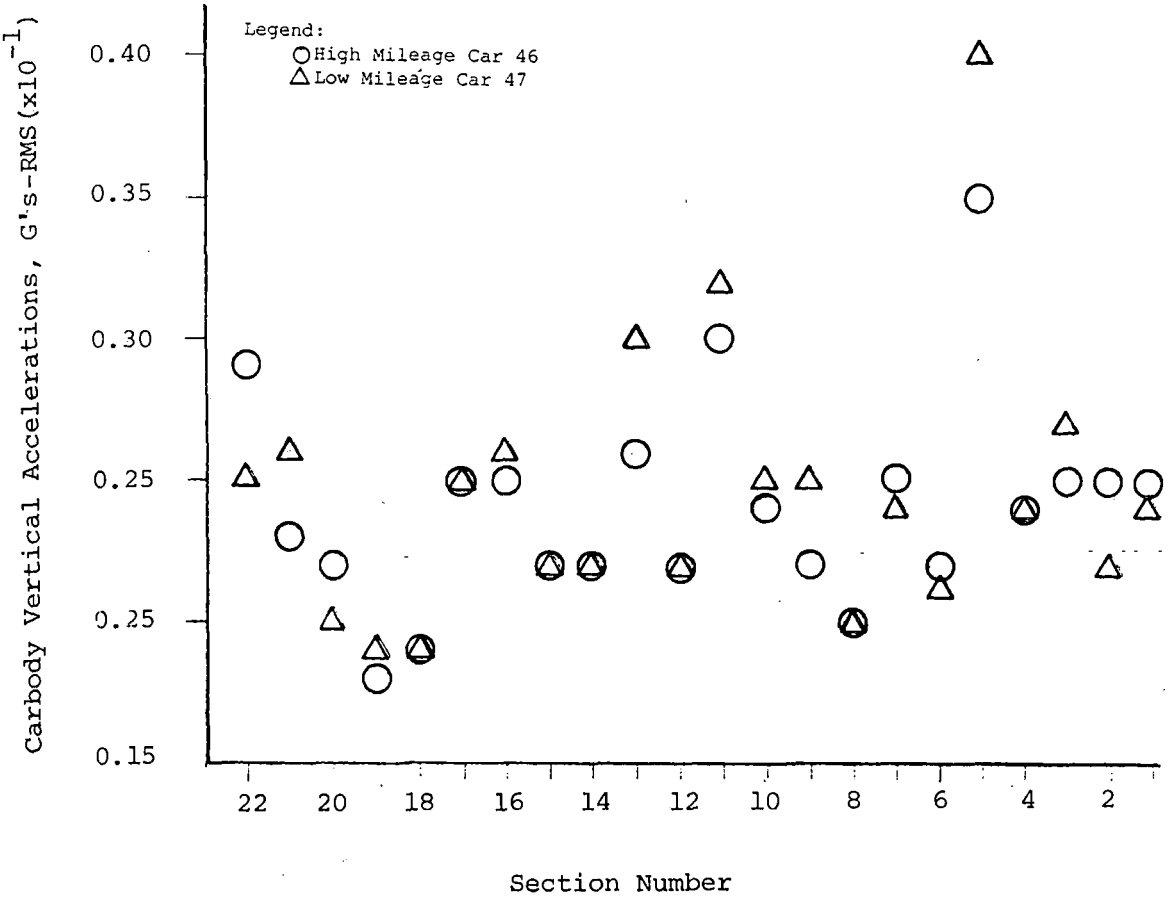

FIGURE 4-10. CARBODY VERTICAL ACCELERATIONS VS. SECTION.

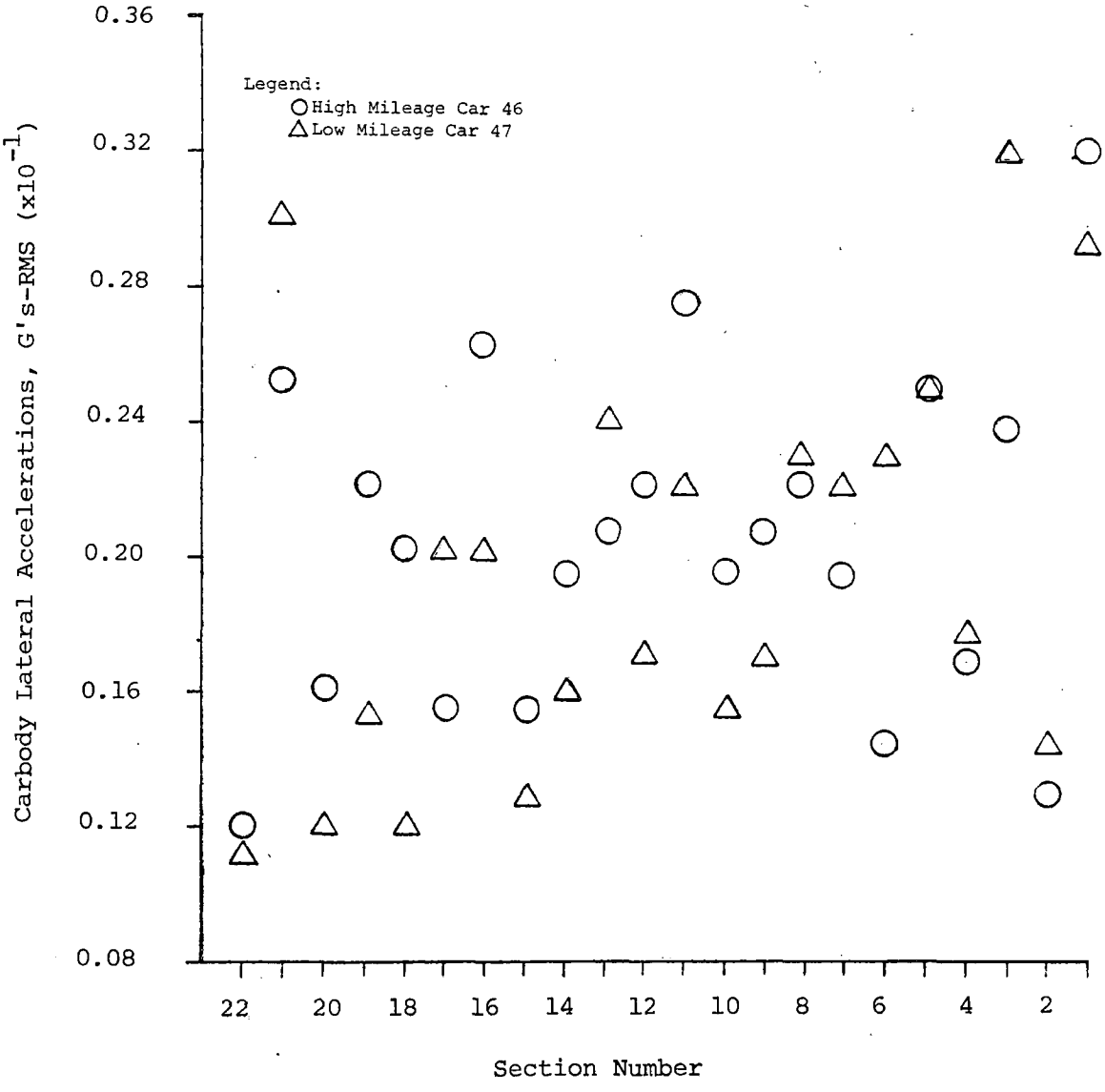

FIGURE 4-11. CARBODY LATERAL ACCELERATIONS VS. SECTION.

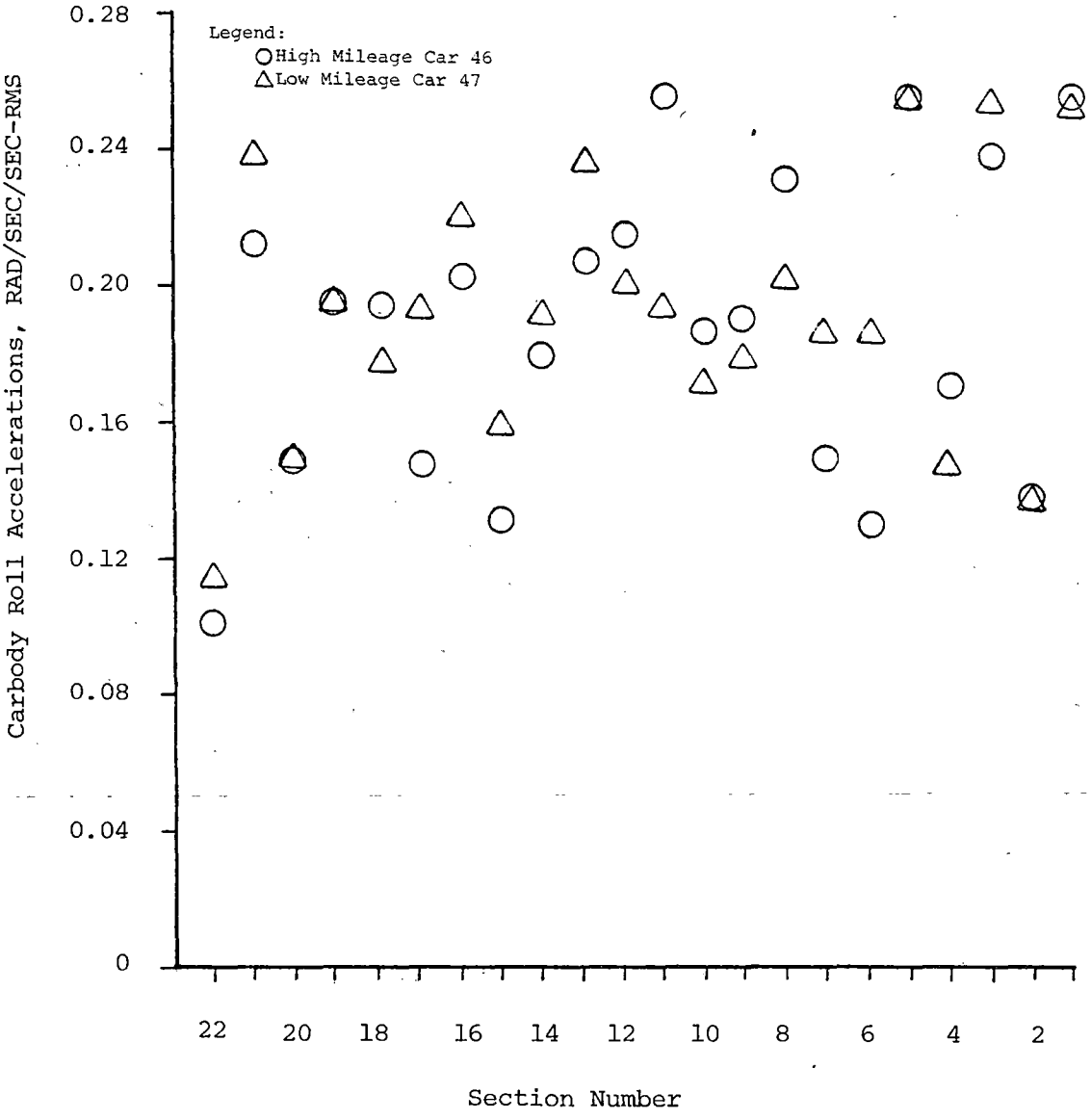

FIGURE 4-12. CARBODY ROLL ACCELERATIONS VS. SECTION.

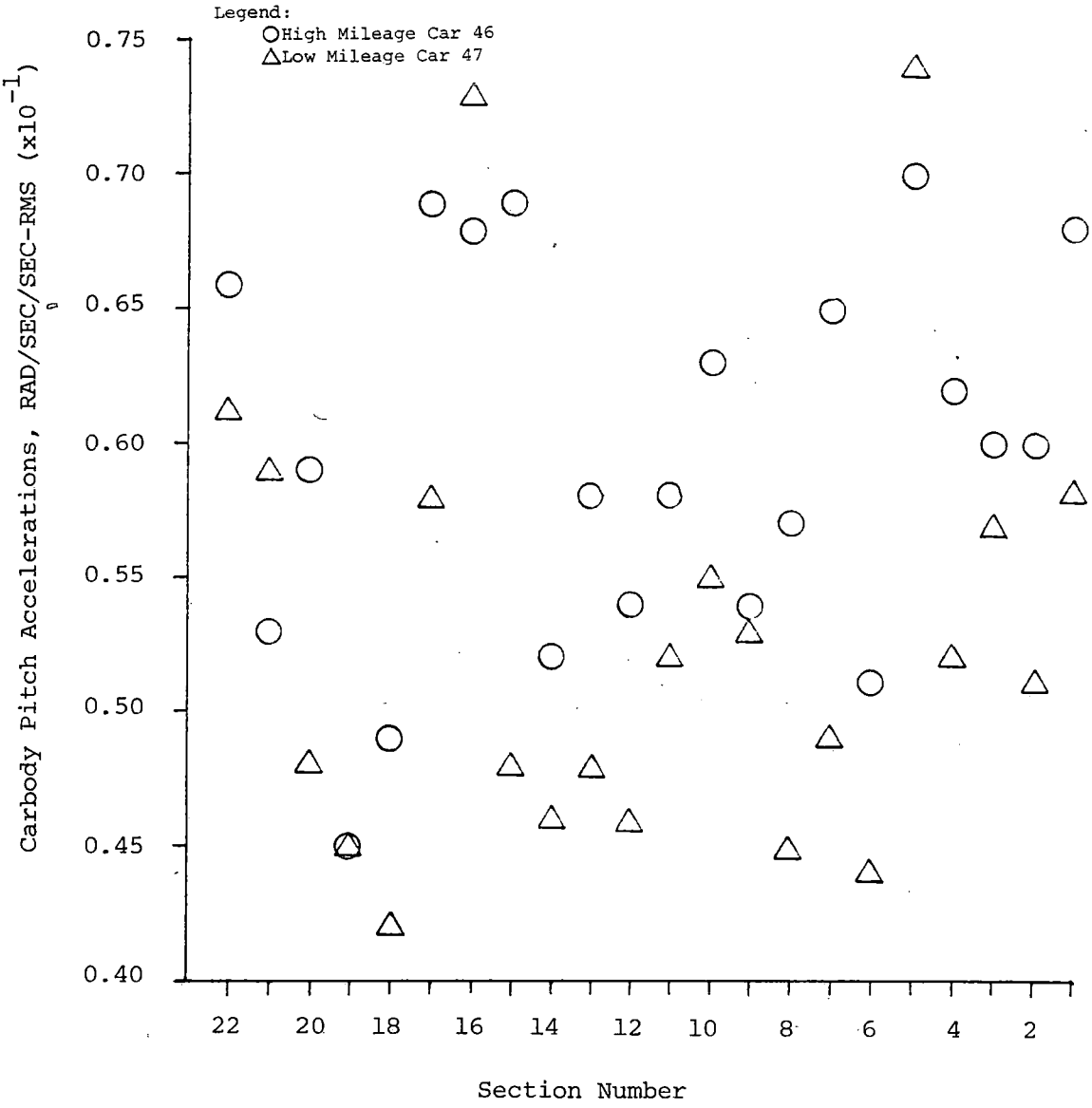

FIGURE 4-13. CARBODY PITCH ACCELERATIONS VS. SECTION.

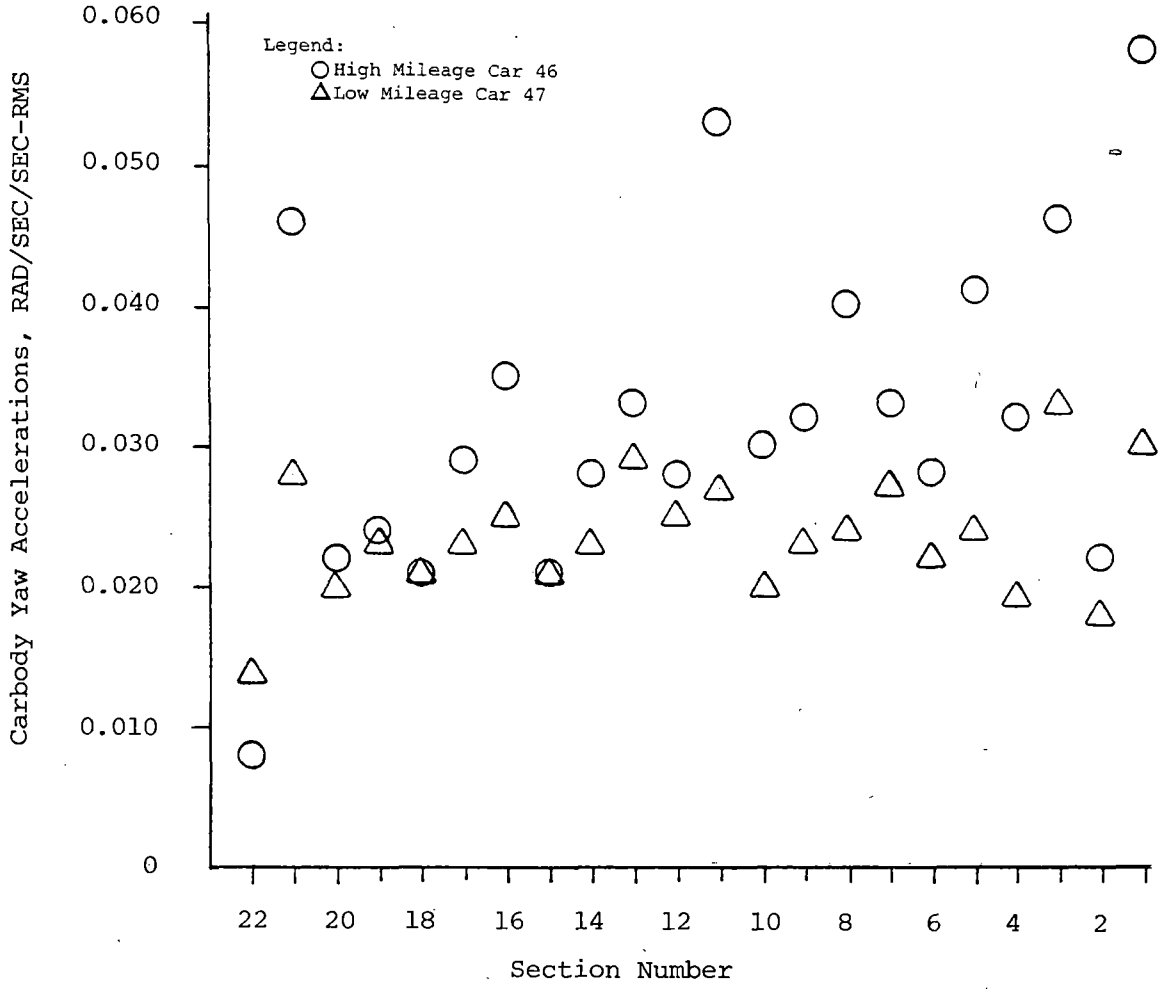

FIGURE 4-14. CARBODY YAW ACCELERATIONS VS. SECTION.

TABLE 4-3. CARBODY ACCELERATION STATISTICS.

	CARBODY									
	46	47	46	47	46	47	46	47	46	47
Section	G's Vertical		G's Lateral		Rad/Sec^2 Roll		Rad/Sec^2 Pitch		Rad/Sec^2 Yaw	
01										
St Dev	0.02	0.02	0.03	0.03	0.29	0.26	0.07	0.06	0.06	0.03
95%	0.05	0.05	0.07	0.07	0.63	0.51	0.13	0.12	0.13	0.06
99%	0.07	0.06	0.11	0.10	1.01	0.88	0.19	0.16	0.23	0.09
RMS	0.02	0.02	0.03	0.03	0.27	0.25	0.07	0.06	0.06	0.03
02										
St Dev	0.02	0.02	0.01	0.01	0.15	0.14	0.06	0.05	0.02	0.02
95%	0.05	0.04	0.02	0.03	0.29	0.26	0.12	0.10	0.05	0.04
99%	0.06	0.06	0.03	0.04	0.39	0.37	0.15	0.13	0.06	0.04
RMS	0.02	0.02	0.01	0.01	0.14	0.14	0.06	0.05	0.02	0.02
03										
St Dev	0.02	0.03	0.03	0.03	0.25	0.27	0.06	0.06	0.05	0.03
95%	0.05	0.05	0.05	0.07	0.50	0.53	0.13	0.12	0.10	0.07
99%	0.07	0.07	0.07	0.10	0.72	0.76	0.17	0.16	0.15	0.10
RMS	0.02	0.03	0.02	0.03	0.25	0.26	0.06	0.06	0.05	0.03
04										
St Dev	0.02	0.02	0.02	0.02	0.20	0.16	0.06	0.05	0.03	0.02
95%	0.05	0.04	0.03	0.04	0.31	0.32	0.11	0.11	0.07	0.04
99%	0.06	0.06	0.05	0.04	0.38	0.43	0.15	0.15	0.10	0.05
RMS	0.02	0.02	0.02	0.02	0.16	0.15	0.06	0.02	0.03	0.02

TABLE 4-3. CARBODY ACCELERATION STATISTICS, CONTINUED.

	CARBODY									
	46	47	46	47	46	47	46	47	46	47
	G's		G's		Rad/Sec^2		Rad/Sec^2		Rad/Sec^2	
Section	Vertical		Lateral		Roll		Pitch		Yaw	
05										
St Dev	0.03	0.04	0.03	0.03	0.26	0.25	0.07	0.08	0.04	0.02
95%	0.07	0.09	0.05	0.05	0.48	0.54	0.14	0.15	0.09	0.09
99%	0.10	0.12	0.06	0.07	0.67	0.77	0.20	0.19	0.11	0.07
RMS	0.03	0.04	0.03	0.03	0.25	0.25	0.07	0.07	0.04	0.02
06										
St Dev	0.02	0.02	0.02	0.02	0.14	0.18	0.06	0.05	0.03	0.02
95%	0.04	0.04	0.03	0.04	0.27	0.33	0.12	0.09	0.06	0.04
99%	0.06	0.05	0.05	0.06	0.34	0.42	0.16	0.10	0.07	0.05
RMS	0.02	0.02	0.01	0.02	0.13	0.18	0.05	0.04	0.03	0.02
07										
St Dev	0.02	0.02	0.02	0.02	0.16	0.19	0.07	0.05	0.03	0.03
95%	0.05	0.04	0.04	0.05	0.30	0.36	0.14	0.10	0.07	0.05
99%	0.06	0.06	0.05	0.06	0.39	0.50	0.20	0.13	0.09	0.07
RMS	0.02	0.02	0.02	0.02	0.15	0.18	0.07	0.05	0.03	0.03
08										
St Dev	0.02	0.02	0.02	0.02	0.24	0.22	0.06	0.05	0.04	0.03
95%	0.04	0.04	0.04	0.05	0.50	0.41	0.12	0.09	0.09	0.05
99%	0.05	0.05	0.06	0.08	0.60	0.58	0.18	0.15	0.11	0.06
RMS	0.02	0.02	0.02	0.02	0.23	0.21	0.06	0.05	0.04	0.02

TABLE 4-3. CARBODY ACCELERATION STATISTICS, CONTINUED.

	CARBODY									
	46	47	46	47	46	47	46	47	46	47
	Gs		Gs		Rad/Sec^2		Rad/Sec^2		Rad/Sec^2	
Section	Vertical		Lateral		Roll		Pitch		Yaw	
09										
St Dev	0.02	0.02	0.02	0.02	0.20	0.17	0.05	0.06	0.03	0.02
95%	0.04	0.04	0.04	0.04	0.38	0.32	0.11	0.11	0.06	0.04
99%	0.06	0.06	0.05	0.06	0.48	0.42	0.15	0.16	0.10	0.05
RMS	0.02	0.02	0.02	0.02	0.19	0.18	0.05	0.05	0.03	0.02
10										
St Dev	0.02	0.02	0.02	0.02	0.19	0.17	0.07	0.06	0.04	0.02
95%	0.04	0.05	0.04	0.03	0.38	0.32	0.13	0.12	0.07	0.04
99%	0.06	0.07	0.06	0.05	0.60	0.44	0.19	0.17	0.14	0.06
RMS	0.02	0.02	0.02	0.02	0.18	0.16	0.06	0.06	0.03	0.02
11										
St Dev	0.03	0.03	0.03	0.02	0.28	0.20	0.06	0.05	0.06	0.03
95%	0.06	0.07	0.06	0.05	0.56	0.38	0.12	0.11	0.12	0.05
99%	0.08	0.09	0.09	0.07	0.79	0.53	0.15	0.14	0.19	0.07
RMS	0.03	0.03	0.03	0.02	0.27	0.20	0.06	0.05	0.05	0.03
12										
St Dev	0.02	0.02	0.02	0.02	0.22	0.21	0.06	0.05	0.03	0.03
95%	0.04	0.04	0.04	0.04	0.43	0.39	0.11	0.09	0.06	0.05
99%	0.05	0.05	0.05	0.05	0.71	0.51	0.15	0.13	0.08	0.06
RMS	0.02	0.02	0.02	0.02	0.22	0.21	0.05	0.04	0.03	0.03

TABLE 4-3. CARBODY ACCELERATION STATISTICS, CONTINUED.

	CARBODY									
	46	47	46	47	46	47	46	47	46	47
	G's		G's		Rad/Sec^2		Rad/Sec^2		Rad/Sec^2	
Section	Vertical		Lateral		Roll		Pitch		Yaw	
13										
St Dev	0.03	0.03	0.02	0.03	0.21	0.23	0.06	0.05	0.04	0.03
95%	0.05	0.06	0.04	0.05	0.42	0.45	0.12	0.10	0.07	0.06
99%	0.07	0.08	0.05	0.07	0.54	0.57	0.16	0.14	0.10	0.08
RMS	0.02	0.03	0.02	0.02	0.21	0.23	0.06	0.05	0.03	0.03
14										
St Dev	0.02	0.02	0.02	0.02	0.20	0.20	0.05	0.05	0.03	0.02
95%	0.04	0.04	0.04	0.03	0.35	0.37	0.11	0.09	0.06	0.05
99%	0.06	0.06	0.06	0.05	0.57	0.50	0.15	0.12	0.13	0.06
RMS	0.02	0.02	0.02	0.02	0.18	0.19	0.05	0.05	0.03	0.02
15										
St Dev	0.02	0.02	0.02	0.01	0.14	0.16	0.07	0.05	0.02	0.02
95%	0.04	0.04	0.03	0.03	0.27	0.31	0.14	0.10	0.04	0.04
99%	0.05	0.05	0.04	0.05	0.33	0.40	0.17	0.12	0.08	0.06
RMS	0.02	0.02	0.02	0.01	0.14	0.16	0.07	0.05	0.02	0.02
16										
St Dev	0.02	0.02	0.03	0.02	0.21	0.24	0.07	0.07	0.04	0.03
95%	0.04	0.04	0.05	0.05	0.43	0.44	0.14	0.14	0.08	0.06
99%	0.06	0.06	0.08	0.07	0.76	0.63	0.19	0.18	0.12	0.07
RMS	0.02	0.02	0.03	0.02	0.20	0.22	0.07	0.07	0.04	0.03

TABLE 4-3. CARBODY ACCELERATION STATISTICS, CONTINUED.

	CARBODY									
	46	47	46	47	46	47	46	47	46	47
Section	G's Vertical		G's Lateral		Rad/Sec^2 Roll		Rad/Sec^2 Pitch		Rad/Sec^2 Yaw	
17										
St Dev	0.02	0.02	0.02	0.02	0.17	0.20	0.07	0.06	0.03	0.02
95%	0.05	0.05	0.03	0.05	0.34	0.39	0.14	0.12	0.07	0.05
99%	0.06	0.06	0.05	0.08	0.53	0.58	0.19	0.16	0.11	0.07
RMS	0.02	0.02	0.02	0.02	0.16	0.19	0.07	0.06	0.03	0.02
18										
St Dev	0.02	0.02	0.02	0.01	0.20	0.18	0.05	0.04	0.02	0.02
95%	0.04	0.03	0.04	0.03	0.36	0.32	0.10	0.09	0.04	0.04
99%	0.05	0.05	0.05	0.04	0.47	0.38	0.15	0.11	0.07	0.05
RMS	0.02	0.02	0.02	0.01	0.19	0.18	0.05	0.04	0.02	0.02
19										
St Dev	0.02	0.02	0.02	0.02	0.20	0.19	0.05	0.05	0.03	0.02
95%	0.03	0.04	0.04	0.03	0.35	0.34	0.09	0.09	0.05	0.04
99%	0.05	0.05	0.05	0.04	0.42	0.44	0.12	0.14	0.07	0.05
RMS	0.02	0.02	0.02	0.02	0.20	0.19	0.05	0.05	0.02	0.02
20										
St Dev	0.02	0.02	0.02	0.01	0.20	0.16	0.06	0.05	0.02	0.02
95%	0.04	0.04	0.03	0.02	0.31	0.30	0.12	0.10	0.05	0.04
99%	0.05	0.05	0.04	0.03	0.40	0.37	0.17	0.13	0.06	0.05
RMS	0.02	0.02	0.02	0.01	0.16	0.16	0.06	0.05	0.02	0.02

TABLE 4-3. CARBODY ACCELERATION STATISTICS, CONTINUED.

	CARBODY									
	46	47	46	47	46	47	46	47	46	47
Section	G's Vertical		G's Lateral		Rad/Sec^2 Roll		Rad/Sec^2 Pitch		Rad/Sec^2 Yaw	
21										
St Dev	0.02	0.03	0.03	0.03	0.21	0.23	0.06	0.06	0.05	0.03
95%	0.04	0.05	0.05	0.06	0.39	0.44	0.12	0.12	0.11	0.06
99%	0.05	0.06	0.09	0.10	0.57	0.60	0.15	0.15	0.17	0.08
RMS	0.02	0.02	0.03	0.03	0.22	0.24	0.05	0.06	0.05	0.03
22										
St Dev	0.03	0.02	0.01	0.01	0.11	0.12	0.07	0.06	0.02	0.02
95%	0.05	0.04	0.03	0.03	0.21	0.33	0.14	0.12	0.04	0.03
99%	0.06	0.06	0.03	0.05	0.33	0.36	0.19	0.16	0.08	0.05
RMS	0.03	0.02	0.01	0.01	0.10	0.12	0.07	0.06	0.02	0.01

Likewise, in the roll mode, both cars seemed to perform in a similar manner. In the pitch mode, however, car 47 clearly showed superior performance, yielding lower yaw accelerations in 18 of the 22 test sections. In general, it can be concluded that car 47 produced overall lower carbody accelerations or a superior ride performance.

To evaluate the effect of track structure on carbody mode vibrations, figures 4-10 through 4-14 require more analysis in order to make observations similar to those made for truck accelerations. First, each mode was qualitatively analyzed for those test sections which produced either relatively high or low accelerations. Then, a tabulation was made of the number of modes for which a given test section was determined to produce either a relatively high or low acceleration. The results of this analysis showed that Sections 15, 18, 19, 20, and 22 produced relatively low carbody accelerations for three or more modes. Similarly, it was found that Sections 01, 05, and 21 produced relatively high carbody accelerations for three or more modes.

Tangent sections that were free of obstructions such as frogs, turn-outs, or guard rails were those sections over which carbody accelerations were relatively low. Section 19 is composed of two 300-ft spirals. Sections 01 and 21 are short sections with a turnout in each. These sections caused relatively high truck mode accelerations from a single acceleration impulse. Section 16 is similar, but the turnout is glued as opposed to the standard and welded turnouts in Sections 01 and 21, respectively. Carbody mode accelerations were the highest on Section 05, which has bonded joints. These joints are unsupported and their condition probably caused a resonance in the carbody suspension at 30 mi/h.

In conclusion, carbody mode accelerations are useful in determining the relative ride performance of hopper cars. During this phase of the dynamic hopper car test, car 47 produced the better overall ride performance. It was also observed that lower carbody accelerations were produced on tangent track free of turnouts, frogs, and guard rails, while higher accelerations were incurred at turnouts and over rail with unsupported joints. Note that this conclusion was not the result of lower mileage but of different car characteristics.

4.3 WHEEL FORCES

In the areas of rail safety and track maintenance, the measurement of force at the wheel/rail interface is of primary importance; this force is intimately connected with the phenomena of gage widening, rail rollover, and wheel climb. Force is a vector quantity possessing both magnitude and direction. It is made up of components in an orthogonal coordinate system. In the study of wheel/rail forces, the most important forces are those in the lateral and vertical directions. The simplest and perhaps most useful means of reducing this vector quantity to a scalar quantity is to define a new parameter as the ratio of lateral to vertical force, denoted L/V. This may be thought of as a normalized force whose magnitude is equal to the tangent of the acute angle between the local vertical and the wheel/rail force. At sufficiently large values of L/V, the force vector will lie outside the rail base. Prolonged force of this magnitude can result in rail rollover.

Lateral wheel forces and L/V ratios were tabulated and plotted versus section number. The L/V ratios were calculated based on instantaneous values of lateral forces and averaged (one revolution) vertical forces. A time history of L/V was created and processed in the same manner as the mode accelerations, resulting in an rms value.

The rms lateral wheel forces for both wheels of the trailing axle of the trailing truck were plotted versus test section in figure 4-15 for a speed of 30 mi/h. In addition, table 4-4 is a statistical presentation of both lateral wheel forces and L/V ratios. Figure 4-15 and table 4-4 indicate that the trends in lateral force and L/V ratio were generally similar to those of the truck modes with few exceptions. High* forces were experienced on both wheels for those short sections of track containing turnouts (Sections 01, 16, and 21).

Sections containing curves produced higher force differentials between left and right wheels than did tangent sections. It was interesting to note that the curve in Section 07 produced significantly higher forces than the curve in Section 03 although they have the same degree of curvature.

Spirals exiting from a curve exhibit tremendous force differentials. However, spirals entering a curve do not exhibit any significant force differential (as in Sections 02 and 06 going counterclockwise).

Through short tangent sections following curves (Sections 11, 15, and 18), the force difference between wheels was present and similar to the situation seen in curves. If the tangent were long enough to provide sufficient time for the force differential to damp out, then the left and right wheel force on the tangent would be about the same (Sections 09 and 10).

It was observed that the wheel on the high rail produced larger forces than that on the low rail.** This result was anticipated from centrifugal effects which are caused by the vehicle transversing the curve. Characteristics of track construction other than discrete events (turnouts) and curvature had little effect on lateral forces or L/V ratios. For instance, Section 11, which produced some of the highest truck mode accelerations, showed only moderate-to-low rms lateral forces, yet Section 11 was a tangent section containing frogs, guard rails, and jointed rail.

In general, there was good agreement between wheel/rail force measurements and truck mode accelerations. Both types of measurements indicated little dependence on differences in track or roadbed construction techniques. Higher forces were experienced on sections of track containing turnouts, spirals, and curves. Also, forces measured on the wheel on the high rail were higher than on the low rail.

---

* The terms high, moderate, and low are used for comparative purposes in classifying rms forces and do not refer to absolute values of forces.

** The orientation of the instrumented wheelset is such that the left wheel follows the high rail for curves to the right and vice versa.

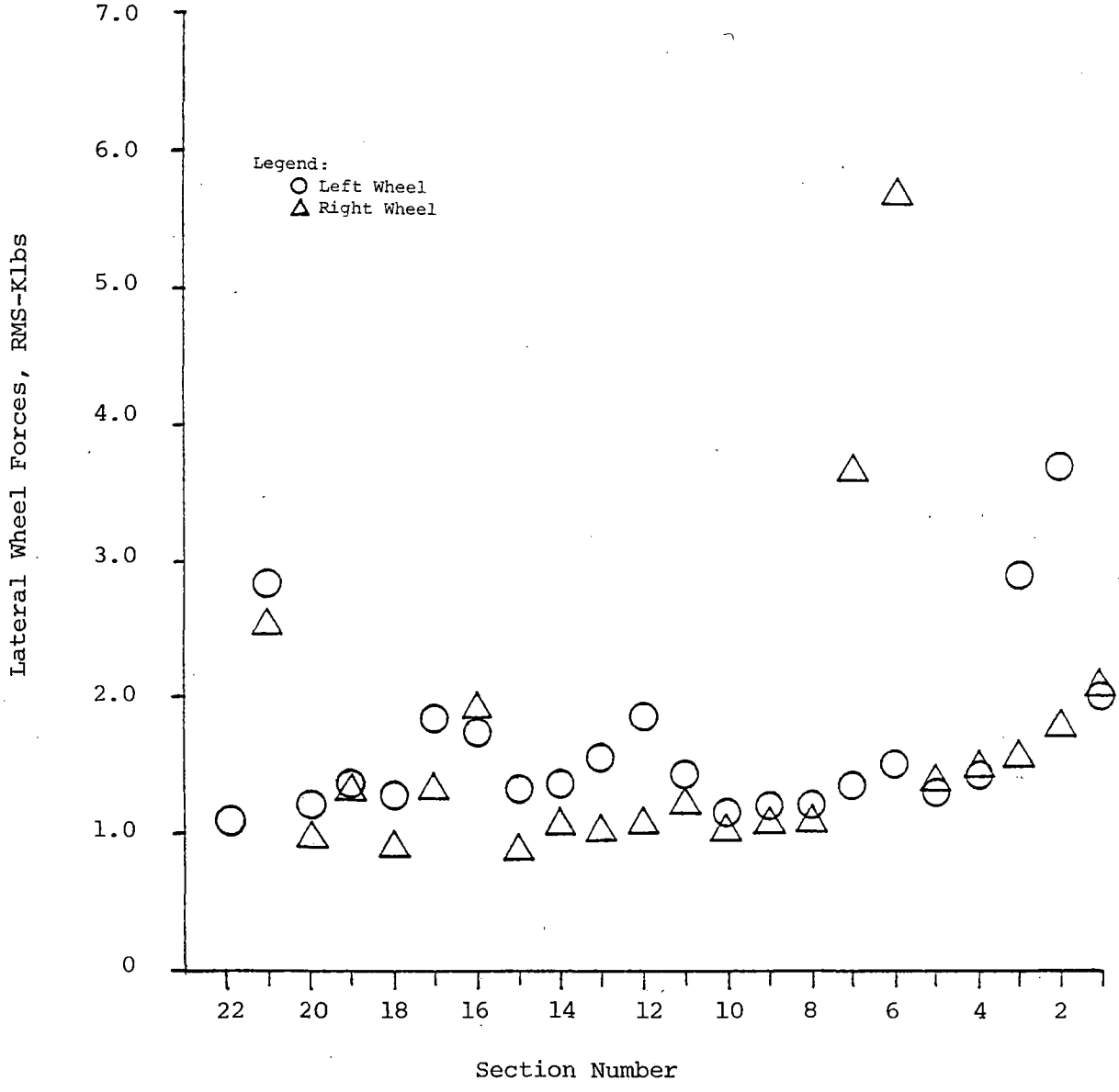

FIGURE 4-15. LATERAL WHEEL FORCES VS. SECTION.

TABLE 4-4. WHEEL FORCE STATISTICS.

Axle No. 1.

	Left Lateral (KLBS)				Left L/V				Right Lateral (KLBS)				Right L/V			
FAST Section	St Dev	95%	99%	RMS	St Dev	95%	99%	RMS	St Dev	95%	99%	RMS	St Dev	95%	99%	RMS
01	2.03	4.36	7.02	1.96	0.09	0.19	0.31	0.08	1.98	4.17	7.22	2.06	0.08	0.17	0.27	0.08
02	2.40	6.59	8.34	3.69	0.11	0.30	0.36	0.16	1.43	3.76	4.35	1.75	0.06	0.15	0.18	0.07
03	1.71	5.23	6.71	2.88	0.07	0.21	0.27	0.11	1.58	3.36	4.98	1.52	0.07	0.14	0.22	0.06
04	1.52	3.10	3.64	1.41	0.06	0.13	0.16	0.05	1.00	2.90	3.50	1.45	0.04	0.13	0.16	0.06
05	1.28	2.49	2.97	1.28	0.06	0.11	0.14	0.05	1.21	2.31	3.90	1.34	0.05	0.10	0.16	0.05
06	1.32	2.83	3.58	1.49	0.06	0.14	0.16	0.07	2.62	8.79	9.70	5.67	0.10	0.34	0.37	0.21
07	1.37	0.78	3.66	1.35	0.07	0.13	0.17	0.06	1.82	7.14	8.43	3.65	0.06	0.26	0.30	0.13
08	1.25	2.43	2.97	1.21	0.06	0.12	0.15	0.06	1.36	3.11	4.24	1.08	0.05	0.12	0.16	0.04
09	1.20	2.25	2.96	1.20	0.05	0.10	0.12	0.05	1.07	2.00	3.19	1.05	0.05	0.09	0.13	0.04
10	1.20	2.18	3.17	1.15	0.05	0.10	0.14	0.05	1.04	2.05	2.96	1.00	0.04	0.09	0.12	0.04
11	1.40	2.68	3.82	1.39	0.06	0.12	0.17	0.06	1.27	2.32	3.99	1.22	0.05	0.10	0.17	0.05
12	1.55	3.63	4.65	1.85	0.07	0.17	0.21	0.08	1.12	2.20	3.48	1.05	0.05	0.09	0.15	0.04
13	1.39	3.07	3.94	1.54	0.06	0.13	0.17	0.06	1.02	1.99	2.74	1.00	0.05	0.08	0.11	0.04
14	1.36	2.70	3.52	1.36	0.06	0.11	0.14	0.05	1.06	2.21	3.13	1.05	0.05	0.10	0.13	0.04
15	1.40	2.38	4.86	1.33	0.06	0.10	0.20	0.05	0.91	1.57	3.69	0.82	0.04	0.07	0.15	0.03
16	1.76	3.59	4.78	1.73	0.08	0.15	0.22	0.07	1.64	4.10	6.47	1.89	0.07	0.16	0.26	0.08
17	2.13	5.22	6.82	1.82	0.09	0.22	0.29	0.07	1.42	3.30	4.97	1.30	0.06	0.14	0.21	0.05
18	1.27	2.50	3.05	1.26	0.06	0.11	0.14	0.05	0.90	1.77	2.23	0.89	0.04	0.08	0.10	0.03
19	1.34	2.54	3.15	1.34	0.06	0.11	0.13	0.05	1.33	2.74	3.87	1.36	0.06	0.12	0.16	0.05
20	1.20	2.30	2.83	1.21	0.05	0.10	0.12	0.05	0.93	1.73	2.32	0.90	0.04	0.07	0.10	0.03
21	2.54	5.94	7.02	2.79	0.11	0.25	0.31	0.11	2.01	5.49	6.83	2.51	0.08	0.22	0.28	0.10
22	1.04	1.97	2.56	1.02	0.05	0.08	0.11	0.04	0.86	1.68	2.59	0.83	0.04	0.07	0.11	0.03

4.4 TRANSMISSIBILITY

In order to assess the effect of component wear on the ride performance of the cars under study, the transmissibility between axles and carbody modes was determined. At a given speed, the system made up of the carbody, the truck, and the suspension elements was assumed to be linear. This assumption allowed for linear techniques to be employed in the calculation of the transfer function between axle and carbody modes. The transfer function can be thought of as a characterization of the hopper car system which is independent of the track condition over which the car was operated. Future changes in transfer function characteristics with accumulated mileage can therefore be directly attributed to changes in the elements of the system.

A transfer function is obtained by forming the ratio of output amplitude to input amplitude. For the purposes of the present study, this ratio was formed in the frequency domain using PSD's. As outlined in sections 4.2.1 and 4.2.2, time histories of carbody and truck mode acceleration were obtained. Using a Fast Fourier Transform (FFT), these time histories were transformed into the frequency domain, and the PSD of a given mode acceleration was created by a complex multiplication of the Fourier Transform with its conjugate. The result of this is a spectral distribution with frequency in terms of mean square acceleration or power; hence, the term power spectral density.

The power in each frequency increment of a given carbody mode PSD was then divided by the power in each corresponding frequency increment of a given truck mode PSD. The result of this was the spectral distribution with frequency of the mean square gain factor between a given carbody mode and a given axle mode. The mean square transfer function was thus calculated between the modes indicated by an X in table 4-5.

TABLE 4-5. TRANSFER FUNCTIONS CALCULATED.

	Carbody Modes (Output)				
	Bounce	Lat	Roll	Pitch	Yaw
Bounce	X			X	
Lateral		X			X
Roll			X		

These mean square transfer functions, referred to more simply as transmissibility, were calculated for both of the cars at 10, 20, 30, 40, and 50 mi/h. Transmissibility is discussed in the next section beginning with an analysis of speed dependence.

4.4.1 Speed Dependence

As stated in section 4.4, a hopper car may only be considered linear or nearly so at a given speed. The reasons for this are twofold. First, the geometry of both the trucks and the carbody act as spatial filters, and second, the truck suspension is itself a nonlinear system. These elements are pictured schematically in figure 4-16.

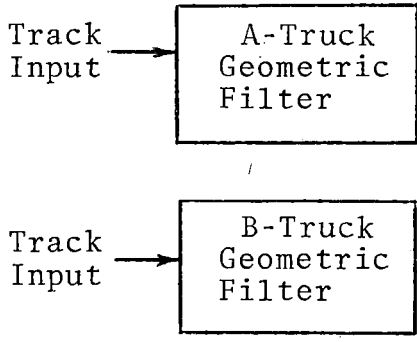
Track
Input
A-Truck
Geometric
Filter
Track
Input
B-Truck
Geometric
Filter

FIGURE 4-16.

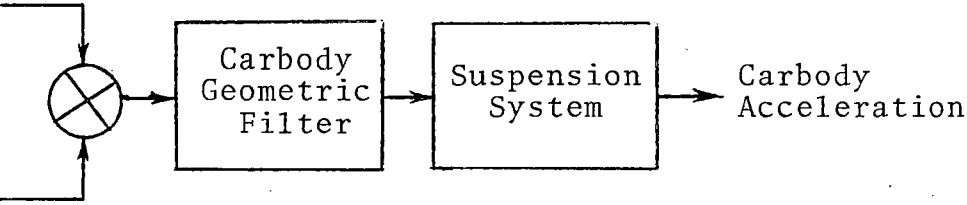

SCHEMATIC DIAGRAM - HOPPER CAR LINEARITY.

In order to see how the geometric filter occurs, the truck is simplified as shown in figure 4-17. The side frame is a rigid beam separating the axles by a distance (ℓ) while the truck traverses a sinusoidal track of amplitude (A) and spatial wavelength (λ).

Based on this two dimensional model, the vertical (lateral) translation F of the bolster is:

$$F(x) = A \cos \frac{\pi \ell}{\lambda} \sin \frac{2\pi x}{\lambda} \quad , \tag{23}$$

where F(x) is the vertical (lateral) translation and x is the distance along the track. Similarly, the pitch (yaw) rotation is:

$$X(x) = \frac{2A}{\lambda} \sin \frac{\pi \ell}{\lambda} \sin\left(\frac{2\pi x}{\lambda}, \frac{\pi}{2}\right) , \tag{24}$$

where X(x) is the angular displacement in pitch (yaw) of the truck bolster.

The terms containing the argument $\pi \ell / \lambda$ are attenuation factors. The spatial wavelength (λ) is related to frequency (f) by the speed (V) written as:

$$\lambda = V/f. \tag{25}$$

Making use of this relation, the argument of the attenuation factors may be written as $\pi \ell f/V$. Thus, it is apparent that the linear and angular displacement are nonlinear functions of axle spacing and speed.

Similar deviations can be made based on truck center spacing. The effect of a geometric filter is to impose a rectified sinusoidal attenuation factor on the transfer function gain, resulting in evenly spaced peaks and valleys in the output PSD. The large difference in axle and truck center spacing will cause two such families of peaks. Based on the truck center spacing and the speed range of interest, the distance between peaks will be approximately 1 Hz; based on axle spacing, this distance will be in the order of 10 Hz. These features will be clearly seen in the results of the transmissibility processing. In addition to these geometric filters, the suspension system of the truck itself is also nonlinear in nature because it had elements such as Coulomb friction dampers and hard or soft springs. Thus, it is apparent that the carbody response in terms of track geometry input will be characterized by a nonlinear transfer function gain or transmissibility.

4.4.2 Transmissibility Results

Transmissibility plots for the high-mileage car (No. 46) and the low-mileage car (No. 47) were generated to include plots of those transfer functions specified in table 4-5 for each of the five speeds. Before proceeding with this discussion, it should be noted that the transfer function for axle-vertical to carbody-pitch and axle-lateral to carbody-yaw represent gains between translational inputs and rotational responses. Therefore, the physical significance of these factors is not immediately obvious. In order to make the transfer function nondimensional, it would be necessary to select a location on the carbody at which a translational acceleration due to pitch (yaw) could be calculated. However, for this study,

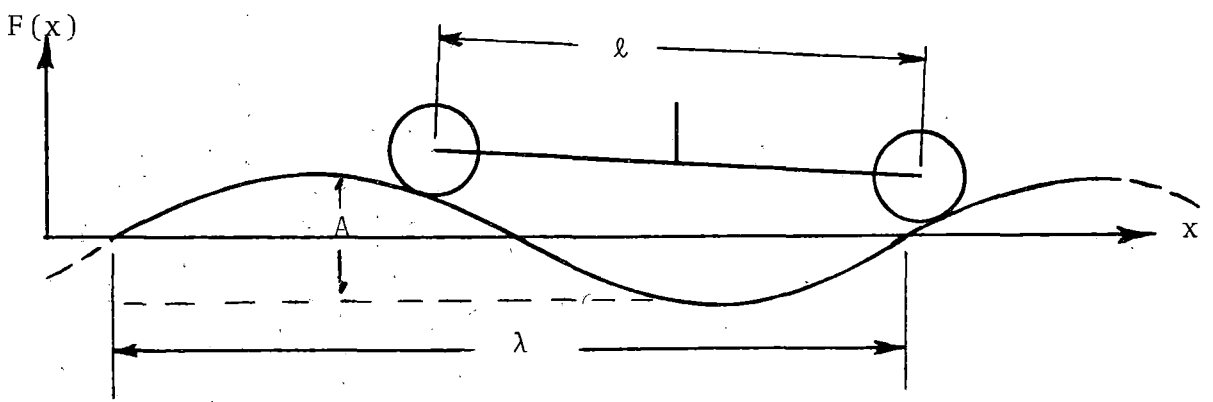

FIGURE 4-17. THE TRUCK GEOMETRIC SPATIAL FILTER.

relative values of transmissibility provide sufficient information for comparative analysis.

A cursory review of the plots verified the nonlinear characteristics of the transfer function with speed. Closer examination revealed the attenuation factors due to axle and truck center spacing. An example of the rectified sinusoidal attenuation factor is shown in figure 4-18.

A qualitative analysis of the transfer functions resulted in the following observations:

- Ratios greater than unity were present in all modes and at most speeds.
- Frequencies at which peaks were observed are somewhat independent of speed. This was particularly evident in the case of vertical and roll transmissibility.
- A subjective comparison of transfer functions for cars 46 and 47 indicates that the characteristics of car 47 are marginally better than those of car 46. Specifically, car 47 demonstrated lower values in the lateral and yaw modes, while those for the vertical roll and pitch modes for both cars were nearly the same.

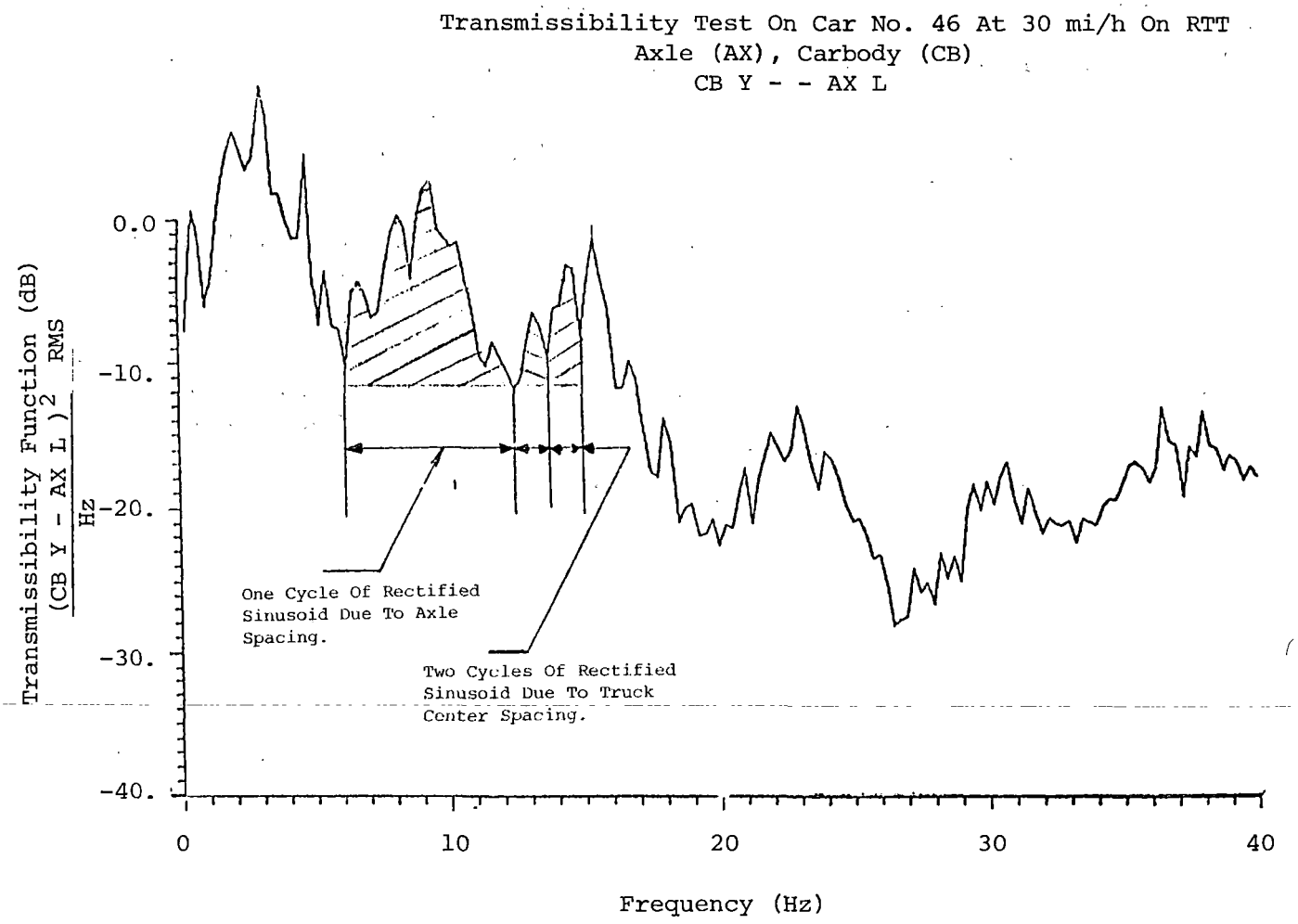

FIGURE 4-18. GEOMETRIC FILTER EFFECTS.

5.0 CONCLUSIONS AND RECOMMENDATIONS

The results of the third dynamic hopper car test presented in this report were directed at quantifying the dynamic response of freight vehicles to different track structures. In addition, these results were used to establish a baseline for future study of the relationship between ride performance and (1) track degradation, (2) vehicle component wear, and (3) vehicle/track system degradation. These latter objectives will be addressed as mileage is accumulated and subsequent test results are obtained.

One basic conclusion of this work is that the instrumentation and data processing techniques developed proved successful in evaluating the dynamic performance of railcars. The use of mode accelerations yielded concise, clear engineering results which correlated well with observed physical phenomena. For example, a comparison of truck mode accelerations for two different trucks has shown that these accelerations can be used to characterize track conditions. These results indicate that truck mode accelerations will be a useful tool in the study of track degradation.

Along these same lines, wheel-to-rail force measurements were found to be reasonable and in general agreement with truck mode accelerations. Although the results of the transmissibility analysis are somewhat more difficult to relate to physical phenomena, these results parallel those obtained from carbody and truck mode acceleration data.

Conclusions related to the objective of quantifying vehicle dynamic response to different track structures are: variations in track structure, such as ballast shoulder width and depth, spiking patterns, tie material, and rail anchors, had little if any effect on truck and carbody accelerations or wheel force. In contrast, curves greater than 4° and discrete events, such as turnouts, had a marked effect on vehicle dynamics. Section 05 of the FAST Track, containing unsupported bonded joints, produced the highest carbody accelerations, while truck mode accelerations over this same section of track were moderate to low.

As mentioned above, comparisons of lateral wheel/rail forces with truck accelerations were in agreement. In addition, it was observed that the high wheel in curves experienced larger forces than did the wheel on the low rail. Physical considerations lend credence to this observation. A second observation was that an appreciable difference in wheel/rail forces was measured in left and right hand curves. The causes of this apparent anomaly were not readily apparent and will require further investigation.

Conclusions related to the objectives of determining the relationship between ride performance and track/vehicle component degradation are: the low-mileage car (No. 47) with ASF Ride Control trucks provided marginally better ride performance than did the high-mileage car (No. 46) with Barber S-2 trucks. The data contained in this report have met the objective of providing the data base necessary for further investigation of the dependence of ride performance on the degradation of track and vehicle components with mileage. Again, it must be noted that the two cars under test (1) had experienced an unknown amount of service prior to FAST usage, (2) are not the same and should not be compared in relation to mileage, and (3) require additional test data to yield results necessary to attain the test objectives.

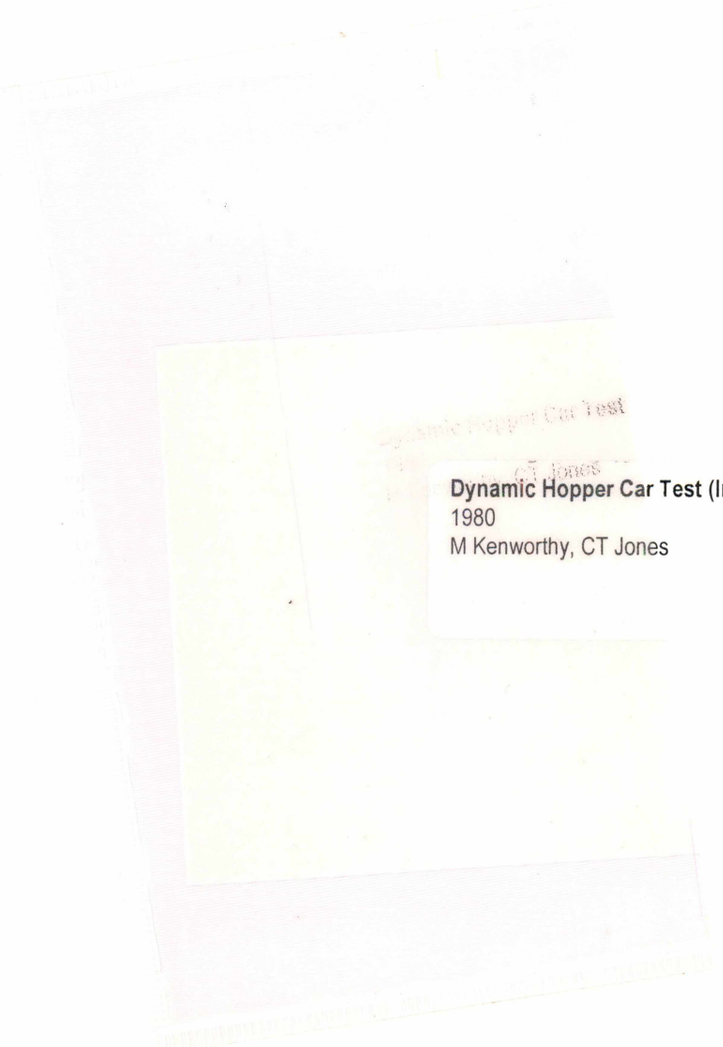

Dynamic Hopper Car Test (Interim Report),
1980
M Kenworthy, CT Jones